



Published in final edited form as:

Mol Neurobiol. 2007 December ; 36(3): 205–223.

Kinetics of Synaptic Transmission at Ribbon Synapses of Rods and Cones

Wallace B. Thoreson

Department of Pharmacology and Experimental Neuroscience, University of Nebraska Medical Center, Omaha, NE 68198-5840, USA

Abstract

The ribbon synapse is a specialized structure that allows photoreceptors to sustain the continuous release of vesicles for hours upon hours and years upon years but also respond rapidly to momentary changes in illumination. Light responses of cones are faster than those of rods and, mirroring this difference, synaptic transmission from cones is also faster than transmission from rods. This review evaluates the various factors that regulate synaptic kinetics and contribute to kinetic differences between rod and cone synapses. Presynaptically, the release of glutamate-laden synaptic vesicles is regulated by properties of the synaptic proteins involved in exocytosis, influx of calcium through calcium channels, calcium release from intracellular stores, diffusion of calcium to the release site, calcium buffering, and extrusion of calcium from the cytoplasm. The rate of vesicle replenishment also limits the ability of the synapse to follow changes in release. Post-synaptic factors include properties of glutamate receptors, dynamics of glutamate diffusion through the cleft, and glutamate uptake by glutamate transporters. Thus, multiple synaptic mechanisms help to shape the responses of second-order horizontal and bipolar cells.

Keywords

Photoreceptor; Synaptic transmission; Glutamate; Calcium; Vesicles; Retina

Vision begins with the transduction of light into membrane potential changes as the result of an enzymatic cascade occurring in the outer segments of rod and cone photoreceptors [1,2]. Light-evoked membrane potential changes are modified by voltage-dependent currents in the inner segment [3] and transmitted to second order bipolar and horizontal cells by changes in release of the neurotransmitter, L-glutamate, from the synaptic terminals of both rods and cones. Because all of the visual information available to downstream retinal neurons must first pass through the photoreceptor synapse, synaptic transmission from photoreceptors has a considerable impact on visual perception. The focus of this review is on mechanisms that shape the kinetics of synaptic transmission at synapses of rods and cones. Additional information on other physiological and anatomical characteristics of photoreceptor ribbon synapses can be found in recent reviews [4–6].

Differences in Rod and Cone Kinetics

Rod and cone photoreceptors are tonically depolarized in darkness with membrane potentials of -35 to -45 mV that allow continuous release of the neurotransmitter, L-glutamate. Light onset causes photoreceptors to hyperpolarize by as much as 30 mV, leading to a reduction in

glutamate release, whereas light offset causes depolarization and an increase in glutamate release. The light responses of cones are five to ten times faster than those of rods [7–9], resulting in a higher flicker fusion frequency for cones than rods [10]. Rod/cone differences in light response kinetics involve rod/cone differences in outer segment Ca^{2+} homeostasis as well as faster inactivation of transduction cascade enzymes in cones [11].

Post-synaptic light responses of cone-driven second-order neurons are also faster than rod-driven responses [12]. The presence of slower light responses in rods would be sufficient to produce slower rod-driven light responses in second-order bipolar and horizontal cells even if rod and cone synaptic kinetics were identical. But the experimental evidence shows that synaptic transmission from rods is slower than transmission from cones. Baylor and Fettiplace [13] found that responses of ganglion cells to depolarizing current injected into cones were threefold faster than rod-driven responses (although these data could also be explained by the rod and cone signals utilizing different synaptic pathways to the ganglion cell). By comparing responses to brief flashes or impulses of light recorded simultaneously from photoreceptors and horizontal cells, Copenhagen and colleagues [9,14] determined that the impulse responses of rod and cone synapses were similar in shape but five to ten times faster for cones, and thus, roughly matched to kinetic differences in their light responses. And finally, direct stimulation of cones evoked much faster post-synaptic responses than stimulation of rods in simultaneously recorded bipolar and horizontal cells [15,16].

Many different factors influence the kinetics of synaptic transmission. Light-evoked hyperpolarization of photoreceptors reduces the open probability of calcium channels, which, in turn, reduces the rate at which glutamate-filled vesicles are released. Depolarization at light offset increases transmembrane calcium influx and stimulates the exocytosis of glutamate. Factors which regulate the rise and fall of intraterminal calcium levels in dark and light therefore play a major role in controlling the kinetics of glutamate release. These include properties of the calcium channels, calcium release from intracellular stores, diffusion of calcium to the release site, buffering, and extrusion from the cytoplasm. Factors which regulate the rise and fall of glutamate in the synaptic cleft also shape synaptic kinetics. These include the diffusion of glutamate from the release site to post-synaptic glutamate receptors and the rate of removal by glutamate transporters. Intrinsic kinetics of glutamate receptors are also important, particularly rates of desensitization and recovery from desensitization. Finally, the rate at which vesicles are replenished also limits the ability of the synapse to track rapid changes in intensity. This review considers the contribution of these different processes to the kinetics of synaptic transmission from rods and cones.

Kinetics of Exocytosis

Various techniques have been employed to measure exocytosis from the photoreceptor synapse, including capacitance measurement techniques that detect the increase in membrane surface area accompanying vesicular fusion, activity-dependent dyes like FM-143 that optically monitor vesicle fusion, and recordings from second-order neurons that detect the post-synaptic currents produced by glutamate released at the synapse. This section begins with a consideration of potential artifacts and limitations in the use of capacitance and synaptic current measurements for the study of exocytosis.

Although capacitance measurements provide a direct measurement of exocytosis, they can be confounded by endocytosis and artifacts arising from large membrane conductance changes. [17]. To avoid large conductance changes produced by the opening of calcium channels, capacitance measurements are typically suspended during the depolarizing test step. Conductance changes arising from calcium-activated tail currents [18,19] also persist after termination of a depolarizing test step. To prevent tail current artifacts, one can inhibit calcium-

activated K^+ currents with tetraethylammonium [19–21] and calcium-activated Cl^- currents with niflumic acid. Niflumic acid is more effective in blocking calcium-activated Cl^- currents in photoreceptors than other Cl^- channel blockers that have been tested including 5-nitro-2-(3-phenylpropylamino)benzoic acid (NPPB), *N*-phenylanthracilic acid, IAA-94, and flufenamic acid. However, niflumic acid does not fully block calcium-activated Cl^- currents in rods even at a concentration of 0.1 mM, and higher concentrations begin to substantially inhibit I_{Ca} [18,22]. Although identification of a more potent and selective blocker of this channel would be useful, the residual tail currents that remain in the presence of niflumic acid do not appear to significantly contaminate capacitance measurements [16,23].

The capacitance change measured after resuming capacitance measurements at the end of a test step yields the net increase in membrane capacitance that occurred during the step. This reflects the exocytotic fusion of vesicles minus any endocytotic retrieval. Countervailing endocytosis during the test step can thus lead to an underestimate of exocytosis. The time course of endocytotic retrieval of vesicles can be determined from the decline in capacitance after the step. Endocytosis in photoreceptors exhibits time constants of a few hundred milliseconds [16,24], and therefore, does not significantly impact measurements of exocytosis evoked with brief test steps. Consistent with this, there is a linear correlation between the amount of release measured using capacitance techniques and release measured by recording the post-synaptic current with test steps up to 1–2 s in duration [16,23]. Endocytosis is inhibited by elevated calcium levels in bipolar cells [25]. Calcium-dependent inhibition of endocytosis in photoreceptors would explain why capacitance measurements appear to provide a reliable measure of exocytosis from photoreceptors even with test steps as long as 2 s.

Another way to measure exocytosis is to record post-synaptic currents evoked in second-order horizontal and bipolar cells by stimulating simultaneously recorded pre-synaptic photoreceptors. The kinetics of the transduction cascade employed by mGluR6 in ON bipolar cells is not fully characterized, so analysis of release kinetics in paired recordings has typically focused on synaptic responses of horizontal and OFF bipolar cells which employ non-NMDA ionotropic glutamate receptors at their synapses (reviewed in [26]). As long as they do not significantly impair voltage clamp, pre-synaptic conductance changes do not significantly impact measurements of release in paired recordings. Instead, one must be concerned about post-synaptic factors that can lead to an underestimate of release: glutamate uptake, glutamate receptor saturation, and receptor desensitization. Glutamate receptors in most horizontal and OFF bipolar cells of the salamander retina are of the AMPA subtype in which desensitization can be blocked by cyclothiazide. In the presence of cyclothiazide, the charge transfer during the excitatory post-synaptic current (EPSC) is linearly correlated with exocytotic capacitance increases [16,23]. The presence of a glutamate transport inhibitor, TBOA, did not significantly improve this correlation [16]. The linear correlation between pre- and post-synaptic measures of exocytosis indicates that increases in exocytosis produce corresponding increases in post-synaptic responses, which, in turn, suggests that glutamate receptors are not saturated by cleft glutamate levels. Linear convolution of single quantal miniature EPSCs (mEPSCs) with the release rate measured using capacitance techniques in cones accurately reproduced the cone-driven EPSC waveform which is also consistent with the conclusion that glutamate receptors are not saturated [15]. These results suggest that after blocking receptor desensitization, the EPSCs recorded during paired recordings appear to provide a fairly accurate measure of release.

Optical techniques have also been used to measure release from the photoreceptor synapse [27]. The activity-dependent dye, FM1-43, inserts into the outer leaflet of the plasma membrane, allowing it to be endocytosed into synaptic vesicles. After removing the dye from the extracellular medium, dye captured in vesicles remains inside the cell until dye-stained vesicles are exocytosed. The destaining of FM1-43 from the terminal can thus be used to track the fusion of vesicles. Photobleaching experiments with FM1-43 have revealed that vesicles

in photoreceptor terminals are unusually mobile [27]. It should also be possible to apply evanescent wave microscopy techniques to monitor the fusion of individual FM1-43 stained vesicles, as has been done at the bipolar cell synapse [28].

The stimulation of cones evokes a fast, transient EPSC in simultaneously recorded OFF bipolar and horizontal cells (Fig. 1a). Stimulation of rods also evokes a transient EPSC in the same post-synaptic cell studied with cone stimulation, but with a slower and more complex time course involving multiple components (Fig. 1b, c). These differences are intrinsic to the synapse, as EPSCs evoked in a horizontal or OFF bipolar cell by stimulation of a cone are consistently faster than EPSCs evoked in the same post-synaptic cell by stimulation of a rod [15,16]. The cone-driven EPSC rises more quickly, with a time constant averaging 2 ms, and attains its peak earlier than the rod-driven EPSC [15]. There is sometimes an initial component present in rod-driven EPSCs with a short latency similar to the fast component of cone-driven EPSCs (see arrow in Fig. 1b). This fast response component of the rod-driven EPSC is labile and disappears rapidly during recording. It may reflect an intrinsic capability for fast release from rods, although it may also involve output from coupled neighboring cones. Cone-driven EPSCs also decay very rapidly with a time constant averaging 8 ms, whereas the time constant of decay for rod-driven EPSCs averaged 58 ms [15]. Rod-driven EPSCs do not always decay with a single exponential time course, but sometimes exhibit a discrete hump in the later portions of the EPSC (Fig. 1c). As discussed later, slow response components of rod-driven EPSCs involve release evoked by calcium-induced calcium release (CICR) from intracellular stores as well as release from coupled neighboring rods evoked by current passing through gap junctions.

Kinetics of exocytosis from rods and cones were measured by determining the amount of release evoked by test pulses of varying duration using both capacitance and paired recording techniques [16]. Both approaches revealed an initial fast component of release from cones with a time constant of ~ 3 ms followed by a slower and more sustained component ($\tau > 0.5$ s). The amplitude of the depolarization-evoked capacitance increase in hair cells and retinal bipolar cells shows a similar bi-exponential dependence on step duration [29,30]. These two kinetically distinct components are thought to reflect an initial transient burst of release followed by slower sustained release [29,30]. The initial fast burst of release from cones evoked by a strong depolarizing step produces an initial transient inward post-synaptic current, and the slower sustained component of release causes a much smaller maintained inward current (Figs. 1 and 3). Capacitance and paired recording techniques also revealed both fast and slow ($\tau > 1$ s) components to release from rods, but the initial component was much slower than for cones ($\tau \sim 45$ ms for steps to -10 mV, $\tau \sim 20$ ms for steps to -30 mV) [16]. This slower initial rate of release accounts for the slower rise of rod-driven EPSCs compared to cone-driven EPSCs [15].

To analyze the contribution of release kinetics to shaping post-synaptic responses, release rates measured with capacitance techniques were convolved with averaged mEPSC waveforms. Convolution of cone release rates with mEPSCs accurately reproduced the waveform of the cone-driven EPSC, and convolution of rod release rates with mEPSCs produced a slower EPSC waveform similar, although not identical, to the actual rod-driven EPSC [15]. This indicates that differences in the rates of exocytosis at rod and cone synapses are responsible for much of the difference in the kinetics of rod- and cone-driven EPSCs. Rod-driven EPSCs were often a bit slower than the waveform predicted by convolution due, in part, to contributions to the EPSC by glutamate released from gap junctionally coupled rods [15].

Light responses of cones increase linearly with small increases in light intensity over the first 10% of the total dynamic range [31]. Bipolar cells respond linearly to small sinusoidal modulations of light intensity ($< 10\%$) about a mean level [32], whereas linearity of horizontal

cell responses is maintained over a larger range of intensities [33]. This indicates that for small intensity changes resulting in small changes in release, processes regulating transmission at the photoreceptor synapse (e.g., I_{Ca} , calcium-dependence of exocytosis, glutamate receptor binding, etc.) remain linear. Furthermore, the finding that responses to incremental and decremental steps of light are mirror images of one another suggests that the processes controlling the rate at which synaptic exocytosis declines at light onset mirror those controlling the increase in exocytosis at light offset. For small intensity changes, it is therefore likely that intracellular calcium levels rise and fall with similar rates at light offset and onset. Responses of bipolar and horizontal cells become increasingly non-linear at higher light intensities. In addition to the sigmoidal intensity/response relationship of the photoreceptor voltage response, this non-linearity also is a consequence of the sigmoidal voltage dependence of I_{Ca} and other nonlinearities in release.

The rate of release maintained by photoreceptors in darkness has been estimated in various ways. Fluctuation analysis of post-synaptic currents in cone-driven OFF bipolar cells of the turtle retina yielded rates of 20–80 vesicles/s/ribbon [34] and mean/variance analysis of ON cone bipolar cell responses of mouse retina yielded a rate of 18 vesicles/s/ribbon [35]. Measurements of FM1-43 destaining suggest an even lower rate of release from lizard cones of ~10 vesicles/s/ribbon in darkness [36]. These results indicate that the entire range of cone light responses is encoded by rather modest changes in release rate. The need to discriminate small changes in release rate to detect small changes in intensity presents a challenge for post-synaptic neurons, particularly if quantal release obeys Poisson statistics [37,38]. Cones may overcome this difficulty by using multiple ribbons (e.g., >50/cone in peripheral cones of primate retina) [39] to encode changes in intensity [5]. The presence of multiple ribbons can amplify release and average out local fluctuations. Mammalian rods, however, have only two ribbons [40]. To permit reliable post-synaptic detection of single photon events, Schein and Ahmad [37] hypothesized that exocytosis at individual release sites may be more regular than predicted by Poisson statistics. The timing of individual mEPSCs recorded from horizontal or OFF bipolar cells is consistent with a Poisson distribution [15,41], but this may reflect the presence of multiple uncorrelated synaptic release sites rather than Poisson release processes operating at each individual release site.

Photoreceptor Coupling

In the amphibian retina, there is strong gap junctional coupling among neighboring rods, as well as direct coupling between rods and cones [42]. Mammalian retina also exhibits inter-photoreceptor coupling, including weak rod–rod coupling [43]. Photoreceptor coupling is mediated by connexons containing Cx36 [44]. Coupling can improve the signal to noise ratio, extend the dynamic range of the rod synapse, and enhance boundary detection by cones [43, 45–47]. Coupling also influences the kinetics of post-synaptic responses by contributing to band pass filtering at rod synapses [48]. The coupling among rods allows hyperpolarizing current to spread from one rod to its neighbors, and thereby, activate hyperpolarization-activated cation (I_h) currents that lead to rebound membrane depolarization [49]. These negative feedback effects are more pronounced at low frequencies because activation of I_h is relatively slow, and thus, acts as a high-pass filter. In addition to I_h effects, the net increase in membrane surface area added by gap junctional coupling among rods contributes to low pass filtering [44]. Modeling suggests that rod–rod coupling accounts for as much as half of the high pass filtering and a smaller fraction of the low pass filtering observed at the rod synapse [48]. Consistent with low pass filtering by gap junctions, blocking gap junctions with carbenoxolone preferentially reduces slower components of the EPSC evoked by depolarizing steps applied to rods [15]. In mammalian retina, spread of depolarizing current through gap junctions into neighboring cones produces a slow, second component in the cone-driven EPSC [50]. Rods also couple to cones, sometimes quite strongly, and the spread of depolarizing

current from one photoreceptor cell type to another can also contribute to shaping post-synaptic responses [43,51]. Although gap junction coupling contributes to slow response components in the rod-driven EPSC, coupling is not entirely responsible for the slow kinetics of exocytosis from amphibian rods, as slow release kinetics are also found in single enzymatically isolated rods [16].

Anatomical Features of the Photoreceptor Synapse

Photoreceptor terminals contain many more synaptic vesicles than conventional synapses. Conventional synapses exhibit 10–100 vesicles clustered near the pre-synaptic density, whereas the synaptic terminal of a lizard cone contains about 170,000 vesicles or 7,000 vesicles/ribbon [36]. Furthermore, only ~20% of the vesicles at conventional synapses are in the rapidly recycling and readily releasable pool; most are in the slowly recycling reserve pool [52,53]. By contrast, 85% of the vesicles in photoreceptor terminals are freely mobile and readily participate in release [27,36].

Synaptic vesicles are tethered by fine filaments to plate-like, electron-dense ribbons at the base of the photoreceptor terminal [54,55]. Synaptic ribbons presumably assist in the continuous release of vesicles from photoreceptors [56], although sustained high frequency release has also been observed at conventional synapses [57]. Photoreceptor ribbons are about 35 nm thick, 1–2 μm long, and up to 1 μm high [58,59]. At the base of the ribbon is a trough-like structure known as the arciform density. The ribbon and arciform density sit above an invaginating depression in the photoreceptor membrane called the synaptic ridge [40,54,55,58–63]. The ribbons of mammalian rods wrap around the synaptic ridge to create a distinctive crescent or horseshoe shape [63]. Synaptic ribbons with different shapes but similar molecular features are found in other sensory neurons including hair cells and retinal bipolar cells [4,5,64–67].

In addition to synaptic ribbons, photoreceptors also make flat or basal contacts onto bipolar cells [55,68]. Flat contacts exhibit pre- and post-synaptic paramembranous densities, but lack the clustering of vesicles that characterizes conventional synapses [55]. In mammalian retina, dendrites of most OFF bipolar cells are not positioned directly adjacent to synaptic ribbons but instead contact cones only at flat junctions [50,68]. The lack of direct ribbon contacts onto mammalian OFF bipolar cells prompted the suggestion that they must therefore receive synaptic input from flat contacts despite the paucity of vesicles [69,70]. Evanescent field imaging studies of bipolar cell terminals show that exocytosis can occur at ectopic sites away from the ribbon [28,71]. However, by comparing correlated synaptic events recorded simultaneously from an OFF bipolar cell that makes only flat contacts and a neighboring OFF bipolar cell whose dendrites enter the invagination, DeVries et al. [50] concluded that most, if not all, of the glutamate reaching post-synaptic processes making flat contacts is released at the ribbon.

The initial fast component of exocytosis is thought to reflect release from a readily releasable pool of vesicles tethered to the base of the ribbon and primed for release [72]. Differences in the number and size of ribbons influence the size of this readily releasable pool [5]. Although cone ribbons are generally smaller in size (~1 μm long \times 0.2 μm high in mammals) than rod ribbons (2 μm long \times 0.4 μm in mammals), cone terminals have many more ribbons than rod terminals, and this probably accounts for their larger exocytotic capacitance response [16]. Although differences in ribbon size and number influence the size of the releasable pool of vesicles, it seems unlikely that they influence the speed at which vesicles are released.

Synaptic Proteins

Ribbon and conventional synapses contain many of the same proteins (see [4,6] for reviews). These include SNARE (SNAP receptor) proteins that assist in vesicular fusion: synaptobrevin

(VAMP1 and 2), SNAP-25, and syntaxin [73–82]. The syntaxin-1 isoform present at many conventional synapses is replaced by syntaxin-3 at ribbon synapses [77,80,83]. Munc 18-1 and Munc 13-1, which assist in SNARE assembly and vesicle priming [84], are both present at ribbon synapses [82,85]. RIM proteins bind to a number of other synaptic proteins at the ribbon synapse including Munc 13-1, CAST1, and rab3 proteins involved in synaptic vesicle docking. RIM1 is localized to the ribbon, whereas RIM2 is clustered at the base of the active zone [81,85]. In addition to RIM1 binding, CAST1 binds to bassoon and piccolo [86,87]. Bassoon is found at the base of the ribbon and appears to help anchor it to the active zone [85,88,89]. Piccolo is a cytomatrix protein like bassoon, but it is found at more distal parts of the ribbon than bassoon.

One notable difference with conventional synapses is the absence of synapsins at ribbon synapses [73,90,91]. In conventional synapses, synapsin 1 appears to tether a reserve pool of vesicles to the cytoskeleton near the active zone [92, but see 93]. The absence of synapsin 1 may allow vesicles to be more freely mobile [27]. The ribbon may also help to replace this function of synapsin by tethering vesicles near the release site.

Another notable difference between ribbon and conventional synapses is the presence of the ribbon-specific protein, ribeye. Ribeye is the major protein in the ribbon with an estimated 4,000 ribeye molecules/ribbon in goldfish Mb1 bipolar cells [94]. The tenfold greater surface area of rod ribbons suggests that they may each possess as many as 40,000 ribeye molecules. Ribeye is an alternative transcript of the gene for transcriptional repressor C terminal binding protein 2 (CtBP-2) but also possesses an additional ribbon-specific domain [95]. It is hypothesized that the ribbon-specific domain may self-assemble to form the central scaffold of the ribbon [95]. CtBP-1 is also present at the ribbon [85]. CtBP1 and 2 play roles in the membrane fission of intracellular organelles [96], suggesting possible roles in vesicle cycling at the photoreceptor synapse. A kinesin motor protein, KIF3A, is present at the ribbon and other synapses [97–99]. Although the presence of a motor protein is intriguing, there is no functional evidence that molecular motors are involved in vesicle movement on the ribbon [4].

There are rod/cone differences in synaptic proteins that potentially may contribute to differences in synaptic release kinetics. For example, cone terminals contain SV2A and SV2B, whereas rod terminals contain only SV2B [100]. SV2A interacts with the proposed calcium sensor, synaptotagmin, in a calcium-dependent manner, and SV2B interacts with synaptotagmin in a calcium-independent manner [101,102]. Knockout of SV2A reduces the size of the readily releasable pool of vesicles in hippocampal neurons [103]. Thus, one can hypothesize that the absence of SV2A from rod terminals might lead to a smaller releasable pool and contribute to the smaller exocytotic responses of rods compared to cones [16]. The antiepileptic drug levetiracetam, which binds selectively to SV2A [104], may provide a tool for testing the role of SV2A at cone synapses.

Amphiphysin and clathrin, both involved in endocytosis, are expressed at higher levels in rods than cones [105]. Although the functional consequences of this difference are unclear, higher rates of exocytosis at cone terminals necessitate higher rates of endocytosis, and this may be accomplished by using different endocytotic proteins.

Synaptotagmin I appears to be the low-affinity calcium sensor at most conventional synapses, but the identity of the calcium sensor(s) employed at rod and cone synapses remains in question. Antibodies to synaptotagmin I/II label photoreceptor ribbon synapses in mouse and bovine retina, but do not label photoreceptor synapses in goldfish and salamander. These are instead labeled by antibodies to synaptotagmin III [106,107]. Synaptotagmin III has a much higher affinity for calcium than synaptotagmin I or II, consistent with physiological findings of a high

affinity release mechanism in amphibian rods [23,24]. The apparent presence of synaptotagmin I/II in mammalian rods raises the question of whether they utilize conventional low affinity sensors or the high affinity sensors found in amphibian rods.

It was recently proposed that otoferlin, not synaptotagmin, may be the principal calcium sensor at the ribbon synapse of hair cells [108]. Otoferlin and other members of the FER protein family have C2 domains with high homology to the C2A domain of synaptotagmin III. FER-like proteins are thus also possible candidates to be the calcium sensor at photoreceptor ribbon synapses.

A surprising property of the high affinity release mechanism in amphibian rods is its relatively low cooperativity for calcium binding ($n \leq 3$) compared to the high cooperativity exhibited by low affinity mechanisms at other synapses ($n \geq 4$) [23,109,110]. Cones appear to have a comparable high affinity mechanism [111]. In addition to the high affinity mechanism, amphibian rods and cones also appear to possess a more conventional, low-affinity calcium sensor [112]. The apparent coexistence of high affinity, low cooperativity mechanisms with low affinity, high cooperativity mechanisms in photoreceptor terminals [23,24,112] may reflect the presence of two distinct calcium sensors, as proposed to explain similar results at bipolar cell synapses [25,108,113,114]. However, it is also possible that the photoreceptor synapse employs a single allosteric sensor mechanism similar to that hypothesized to regulate release at the calyx of Held in which submicromolar calcium evokes release with low cooperativity, whereas higher calcium levels evokes release with greater cooperativity [115].

Photoreceptor Calcium Channels

Neurotransmitter release from photoreceptor synapses is calcium-dependent [116] and triggered by calcium influx through calcium channels. Unlike other conventional synapses which rely on N- and P-type calcium channels [117], photoreceptors and other ribbon synapses employ dihydropyridine-sensitive, L-type calcium channels to vary synaptic release in response to changes in membrane potential [118–122]. The main calcium channels present in photoreceptors are CaV1.4 (alpha 1F) and CaV1.3 (alpha 1D). Although there is no evidence that individual photoreceptor cells possess more than one type of calcium channel, different photoreceptors possess different types of calcium channel. Mutations in CaV1.4 cause various forms of incomplete congenital stationary night blindness [123–126], and antibodies to CaV1.4 label mammalian rod terminals [127–129], suggesting that CaV1.4 is the predominant calcium channel in mammalian rods. CaV1.3 antibodies label most cones in the tree shrew retina; the unlabelled subtype appears to be short wavelength-sensitive (S) cones [130,131]. Consistent with different types of calcium channels in different types of cone, I_{Ca} in red-sensitive, large single cones of the salamander retina is enhanced by activation of cAMP-dependent protein kinase (PKA), whereas I_{Ca} in small single cones and rods is inhibited by PKA activation [132]. Antibodies to L-type calcium channels produce punctate labeling at the base of the ribbon that co-localizes with synaptic proteins such as bassoon and ribeye [85,128,133–135]. This is consistent with physiological results demonstrating highly localized sites of calcium influx at the base of the photoreceptor terminal [136]. Freeze fracture electron micrographs show ~500 transmembrane particles clustered beneath the arciform density of each ribbon [60,137]. These particles, described as polyhedral in shape and containing a central dimple, have been proposed to be the calcium channels [60].

Similar to anatomical estimates, physiological estimates comparing single channel and whole cell conductance measurements yield estimates of 400–500 channels/ribbon in the salamander retina [4,17]. However, these physiological estimates were based on the results of Thoreson et al. [138] showing that the properties of photoreceptor calcium channels were similar to L-type calcium channels in other preparations, including a single channel conductance of 22 pS with

Ba²⁺ as the charge carrier and a maximum mean open probability of ~0.1. By contrast, single channel studies of CaV1.4 channels expressed in HEK cells revealed a much smaller single channel conductance of 3.7 pS and lower maximum mean open probability of 0.014 [139]. This would imply a 40-fold larger number of channels per ribbon (16,000–20,000). A substantially lower single channel conductance would reduce both the amount of calcium entering through each open channel and the voltage noise associated with individual channel openings.

L-type calcium channels in photoreceptors and expressed CaV1.4 channels exhibit limited and slowly developing voltage-dependent inactivation [118,140–143]. Photoreceptor Ca²⁺ channels also exhibit unusually slow Ca²⁺-dependent inactivation compared to other calcium channels [118,140]. Minimal inactivation is important for sustaining output at ribbon synapses [122]. CaV1.3 shows calcium-dependent inactivation, but CaV1.4 does not [143], and so, the presence of calcium-dependent inactivation in amphibian rods suggests they may possess CaV1.3 channels. The continued influx of calcium during sustained activation of photoreceptor I_{Ca} at the dark potential can also reduce I_{Ca} by significantly depleting extracellular calcium ions from the synaptic cleft [140]. Because these voltage- and calcium-dependent reductions in I_{Ca} accompanying sustained activation are slow, changes in I_{Ca} produced by brief changes in illumination largely reflect the sigmoidal voltage dependence of I_{Ca} [144].

In addition to pore-forming alpha1 subunits, calcium channels possess accessory beta and alpha2/delta subunits. Knockout of the beta2 subunit, but not beta1, beta3, or beta4 subunits, from mouse retina almost completely abolished both the ERG b-wave and staining for CaV1.4 in the outer plexiform layer. This suggests that the beta2 subunit is the only beta subunit that combines with alpha1 subunits to create functional channels at the photoreceptor synapse [145]. A mutation in the alpha2/delta type 4 subunit results in disordered ribbons, reduced scotopic b-waves, absent photopic b-waves, and a human cone dystrophy, indicating that this accessory subunit is associated with photoreceptor calcium channels, particularly those of cones [146,147].

The calcium-binding protein, CaBP4, can bind to both CaV1.3 and CaV1.4 [148,149]. Mutations in CaBP4 reduced both rod and cone function; the loss of rod function by CaBP4 mutation leads to congenital stationary night blindness [150]. In the absence of CaBP4, expressed CaV1.4 channels exhibit little or no activity at the dark resting potential of -40 mV and thus seem unsuitable for mediating transmission from photoreceptors. However, coexpression of CaV1.4 with CaBP4 shifts the voltage dependence of I_{Ca} to more negative potentials, thereby enhancing its activation at -40 mV and yielding a current that more closely resembles I_{Ca} in vivo [148].

Although rods possess a different type of calcium channel from cones, the voltage dependence and activation kinetics of I_{Ca} in both cell types are similar [4,16,130,132]. I_{Ca} in rods and cones activate with a rapid, bi-exponential time course with time constants of about 1 and 2.5 ms [16,118]. The kinetics of release from bipolar cell terminals is limited by the activation kinetics of I_{Ca} [29], and it seems plausible that I_{Ca} activation kinetics ($\tau_1 \sim 1$ ms, $\tau_2 \sim 2.5$ ms) also limit the fast release component ($\tau = 3$ ms) in cones [16]. The EPSC evoked by pre-synaptic stimulation of rods rises more slowly ($\tau \sim 8$ ms) than does rod I_{Ca} , indicating that the rise time of slower components of the EPSC is not due to slower I_{Ca} kinetics in rods [15]. The faster decay of cone-driven EPSCs compared to rod-driven EPSCs is also not due to faster inactivation of cone I_{Ca} . Because of the slow time course for I_{Ca} inactivation, the EPSCs evoked by pre-synaptic stimulation of both rods and cones decay well before any appreciable decrease in I_{Ca} [15]. The ability of a sustained I_{Ca} in photoreceptors to elicit transient EPSCs in bipolar and horizontal cells is similar to results at the ribbon synapse made by rod bipolar cells onto AII amacrine cells [151].

Diffusional Distances Between Ca²⁺ Channels and Release Sites

The dynamics of synaptic release are influenced by the diffusion and buffering of calcium from the mouth of the calcium channel to the site of release [152]. Fast release at most synapses requires calcium levels above 20 μM . These levels are typically attained only in nano- or micro-domains of high calcium immediately adjacent to individual calcium channels. Release mechanisms with a low affinity for calcium are therefore effectively limited to release from sites close to individual calcium channels. By contrast, the high-affinity release mechanism employed by amphibian rods permits release by submicromolar calcium levels attained far from individual calcium channels [23,24]. This led to the proposal that exocytosis from rod terminals may be regulated by spatially averaged intraterminal calcium levels rather than the high levels attained in calcium microdomains [24]. On the other hand, the biphasic release kinetics of cones are strikingly similar to those of bipolar cells and hair cells in which the initial fast component of release has been shown to be due to release from sites very close to calcium channels [72], suggesting that the fast component of release from photoreceptors also reflects release from sites close to calcium channels. Consistent with control of release by local calcium, computer simulations modeling the transformation of photoreceptor voltage responses into post-synaptic currents in horizontal and OFF bipolar cells also suggest that glutamate release from photoreceptors depends almost instantaneously on I_{Ca} [144]. In this context, it is worth noting that the extremely low single channel conductance of expressed CaV1.4 channels [139] would be expected to produce lower calcium levels beneath individual CaV1.4 channels than found beneath other calcium channels. Perhaps the presence of high-affinity calcium sensors for release from rods is an adaptation to the presence of calcium channels with an unusually low single channel conductance.

Intracellular Calcium Handling

In addition to influx through voltage-gated calcium channels, calcium levels in the synaptic terminal are regulated by release of calcium from intracellular stores, uptake into organelles, buffering, and extrusion from the cell. Contributions of these mechanisms of calcium regulation to synaptic release are considered below; the role of calcium regulation in phototransduction, cell degeneration, and other aspects of photoreceptor function have been reviewed elsewhere [4,153].

Intracellular calcium is stored and released from the endoplasmic reticulum. Ultrastructural studies revealed smooth endoplasmic reticulum in the inner segments and synaptic terminals of photoreceptors [154] capable of accumulating calcium ions [155]. There are two principal mechanisms of calcium release from internal stores: CICR mediated by ryanodine receptors and release mediated by receptors for the second messenger, IP₃ [156]. Immunohistochemical studies indicate that there are type II ryanodine receptors on synaptic terminals of rods and cones [157,158], and there is physiological evidence, discussed further below, that CICR in rod terminals contributes to release [135,159,160]. Antibodies to type 2 IP₃ receptors also label photoreceptor inner segments and terminals, with particularly strong labeling of cones [158, 161]. However, calcium release from stores triggered by IP₃ production in photoreceptors has not been demonstrated, so it is unclear whether IP₃ receptors participate in photoreceptor synaptic transmission.

At low concentrations ($\leq 1 \mu\text{M}$), ryanodine acts as an agonist at ryanodine receptors, but at high concentrations, ryanodine blocks the receptor [162,163]. Activation of ryanodine receptors with caffeine or low concentrations of ryanodine stimulates the release of calcium from intracellular stores in the inner segments and synaptic terminals of rods (Fig. 2; [136,158, 159]). Brief depolarizing steps ($< 200 \text{ ms}$, -70 to -10 mV) applied to voltage clamped rods and cones produce highly localized calcium increases due to influx through calcium channels

clustered close to the ribbons. In rods, lengthening the step duration to 200 ms or greater stimulated a secondary wave of calcium that spread across the synaptic terminal. This secondary wave was blocked by high concentrations of ryanodine introduced into the cell through the patch pipette, suggesting it was mediated by ryanodine receptors and thus resulted from CICR [136].

In the retinal slice preparation, low concentrations of ryanodine stimulate calcium increases in cones, consistent with immunohistochemical evidence for the presence of ryanodine receptors in cones (Fig. 2; [164]). Cones exhibited a more pronounced calcium increase in their somas and inner segments than in the synaptic region at the base of the soma (Fig. 2; [75]). In contrast to the ability of ryanodine to evoke calcium increases in cones in a retinal slice preparation, caffeine failed to evoke calcium increases in isolated cones unless calcium extrusion by the plasma membrane calcium-ATPase (PMCA) was blocked [157]. Krizaj et al. [157] hypothesized that the efficient extrusion of calcium by PMCA in cone terminals intercepts calcium before it can stimulate significant amounts of CICR. Application of depolarizing steps to cones failed to evoke the calcium waves seen in rods, but instead produced only local calcium changes that rapidly diminished upon termination of the test step [164]. A limited contribution of CICR to calcium regulation in cone terminals also is suggested by the finding that high concentrations of ryanodine (50 μ M) had little or no effect on cone-driven EPSCs in three cone/horizontal cell pairs [164]. These results suggest that although rods and cones both possess ryanodine receptors, CICR is a more prominent feature of intracellular calcium regulation in rods.

CICR promotes the spontaneous release of vesicles [165] and has been shown to contribute to synaptic release from the ribbon synapse in vestibular hair cells [166]. Given the presence of release mechanisms with an unusually high affinity for calcium in rod terminals, it is thus perhaps no surprise that the release of calcium from ryanodine-sensitive intracellular stores is also capable of stimulating glutamate release from rods [136,159,160]. In paired recordings from rods and post-synaptic neurons, blocking CICR with high concentrations of ryanodine preferentially reduced later portions of the depolarization-evoked EPSC [136,160]. Consistent with the finding that CICR significantly boosts intraterminal calcium levels when rods are depolarized for at least 200 ms, ryanodine detectably inhibited PSCs evoked by depolarizing steps maintained for at least 200 ms [136]. CICR amplifies and sustains synaptic output from rods, and thereby, contributes to the slower decay of rod-driven EPSCs observed in paired recordings. However, CICR is not the principal reason for slower synaptic kinetics at the rod synapse, as blocking CICR does not convert slow rod-driven EPSCs into fast cone-driven EPSCs or produce fast cone-like release kinetics [136].

Blocking CICR with ryanodine inhibited light-evoked currents more strongly than it inhibited the EPSCs evoked by strong depolarizing test steps in paired recordings. Suryanarayanan and Slaughter [160] suggest that this discrepancy may result from voltage dependence of CICR, as they found that ryanodine blocked a greater fraction of the EPSCs evoked by depolarizing steps to -40 mV (near the dark potential) than EPSCs evoked by stronger depolarization to -20 mV (above the normal physiological range). Cadetti et al. [136] did not find marked voltage dependence and instead proposed that the strong effect on light responses simply reflects the fact that the fractional contribution of CICR increases as rods are maintained for long periods of time in a depolarized state (e.g., in darkness).

From effects of ryanodine on the amplitude distribution of spontaneous mEPSCs, Suryanarayanan and Slaughter [160] concluded that CICR increased the likelihood that two or more vesicles would be released in a coordinated fashion. Evidence for coordinated release has been obtained at hair cell and bipolar cell ribbon synapses [167,168], so one might anticipate similar processes operating at photoreceptor ribbon synapses. In muscle cells,

calcium influx through a calcium channel can activate a spatially restricted cluster of ryanodine receptors resulting in a highly localized calcium spark [169]. Calcium sparks have not been detected in photoreceptor terminals, but the coordinated opening of a handful of ryanodine receptors adjacent to a calcium channel might provide a means for the calcium flux through a single calcium channel to coordinate the release of vesicles from multiple release sites along the ribbon.

In addition to modifying synaptic transmission directly, calcium released from stores also indirectly influences synaptic output by its actions on calcium-dependent ion currents. Calcium-activated chloride currents in photoreceptors are sensitive to caffeine, suggesting that they may be activated by CICR [20]. Because the chloride equilibrium potential in rods is positive to the dark resting potential, activation of these channels results in chloride efflux, and rod depolarization would depolarize rods and might therefore be expected to stimulate release. This mild stimulatory effect, however, is counterbalanced by direct inhibitory effects of chloride efflux on calcium channels [138]. Conversely, stimulation of calcium-activated potassium channels in rod terminals by CICR can enhance I_{Ca} [19].

IP3 and ryanodine receptors are capable of mobilizing calcium from overlapping internal stores [156]. Depletion of intracellular stores triggers the opening of plasma membrane calcium channels that allow calcium to enter the cytoplasm and facilitate store refilling. Transient receptor potential channels (TRPCs) appear to participate in store replenishment and are widely distributed in different cell types [170]. Little is known about the specific distribution and roles played by various TRPC isoforms in photoreceptors, but an antibody to TRPC6 has been shown to label rod cell bodies [171]. Sarco- and endoplasmic reticulum ATPases (SERCA) pump calcium into the ER. Antibodies to the SERCA 2A subtype label photoreceptor inner segments and synaptic terminals, whereas antibodies to SERCA 2B label inner segments but only weakly label terminals [158].

Calcium continuously enters depolarized photoreceptors in darkness. To prevent overload and cell death, this calcium must be buffered and extruded. In the outer segment, calcium is extruded by a Na/Ca exchanger, whereas inner segment and synaptic terminal extrusion relies principally on PMCA [138,158,172,173]. PMCA are concentrated along the flanks of the terminal and appear to be absent from active zones of the ribbon synapse [135,174]. Antibodies to PMCA subtypes 1, 2, and 4 label photoreceptor terminals [158]. PMCA2 has a tenfold higher affinity for calcium than the other subtypes [175], and PMCA2 knockout mice showed pronounced reductions in the amplitude of rod-driven responses with little change in cone-driven components, suggesting that this subtype is particularly important in regulating calcium levels in rod terminals [176].

Extrusion of calcium is relatively slow compared to calcium buffering. Endogenous calcium-binding proteins bind calcium ions at helix-loop-helix (EF hand) motifs. Most calcium-binding proteins function primarily as signaling molecules, but a handful function mainly as calcium buffers (e.g., calbindin, calretinin, and parvalbumin). Calbindin and calretinin are relatively fast buffers, whereas parvalbumin is relatively slow. Calretinin and parvalbumin exhibit relatively high cytosolic mobility, whereas calbindin exhibits relatively low mobility [177]. Cells differ in their expression of these buffers, and these differences presumably have functional consequences. However, there is considerable species variability in the cellular expression of calcium buffers in retinal cells. The only generalization that can be drawn about photoreceptor expression patterns is that cones of most species possess calbindin (a fast, low mobility buffer), whereas calretinin and parvalbumin are less commonly localized to photoreceptors. The extent to which endogenous calcium buffers shape calcium levels at the release site depends on the location, speed, and affinity of the buffers [152,178]. CaBP4 is directly associated with calcium channels and thus ideally positioned to buffer incoming

calcium ions. Calmodulin often associates with calcium channels and, although it is principally considered a calcium signaling protein, can be present at high enough concentrations ($>1 \mu\text{M}$) to buffer physiologically significant amounts of calcium [179]. We still know little about the specific localization and binding constants for different calcium buffers in relation to the calcium microdomains adjacent to calcium channels. Thus, the role of calcium buffers in regulating calcium dynamics and the kinetics of synaptic release from rods and cones remain unclear.

Properties of Glutamate Receptors

The properties of glutamate receptors, particularly desensitization, greatly influence the kinetics of post-synaptic responses. Presynaptic depolarization of cones evokes EPSCs with markedly different kinetics in different classes of cone-driven OFF bipolar cell from the ground squirrel retina [180]. These kinetic differences reflect the presence of different subtypes of AMPA and KA receptors that recover from desensitization at different rates. B3 and B7 types of OFF bipolar cells that possess KA receptors recovered from desensitization many times more slowly than B2 cells that express AMPA receptors [180].

AMPA receptors desensitize nearly ten times faster than KA receptors [181], raising the possibility that the slowly decaying EPSCs observed at rod synapses may be due to the presence of KA receptors. However, the post-synaptic responses at rod and cone synapses of most horizontal and OFF bipolar cells in the salamander retina are mediated primarily by AMPA receptors [15,182,183]. Maple et al. [183] found that AMPA receptors in cone-dominated OFF bipolar cells desensitized more rapidly than AMPA receptors in rod-dominated OFF bipolar cells. Nevertheless, the desensitization kinetics of AMPA receptors in cone-dominated OFF bipolar cells [183] are too slow to account for the rapid decay of cone-driven EPSCs observed with paired recordings [15]. Kim and Miller [184,185] also suggested that rods and cones may contact different types of glutamate receptors based on differences in the efficacy of low affinity glutamate antagonists. However, low affinity antagonists block lower concentrations of glutamate more effectively than high concentrations, and so these results can also be explained by the presence of higher glutamate levels at rod synapses than cone synapses. In bipolar and horizontal cells receiving both rod and cone inputs, the amplitude and kinetic histograms of spontaneously occurring mEPSCs are unimodal and unchanged by reducing release from rods. This provides additional evidence that for a given post-synaptic cell, rods and cone inputs activate glutamate receptors with similar properties [15]. Thus, differences in the response kinetics at rod and cone synapses appear not to reflect different types of glutamate receptors. Instead, as discussed earlier, the kinetic differences between rod- and cone-driven EPSCs are better explained by rod/cone differences in pre-synaptic release kinetics.

Miniature EPSCs arising from the fusion of individual vesicles can be detected in OFF bipolar as well as uncoupled horizontal cells [15,41,186,187]. Although the slow kinetics of the mGluR6 transduction cascade obscures individual mEPSCs, the presence of an underlying quantal structure to ON bipolar cell responses has been inferred from mean variance analysis [35]. Ultrastructural studies show that vesicles in rods (45–50 nm in salamander rods) are slightly larger than those in cones (35–45 nm) [55,188]. However, selectively reducing the spontaneous release of vesicles from rods did not significantly alter the properties of mEPSCs in mixed rod/cone horizontal cells, suggesting that vesicles of rods and cones contain similar amounts of glutamate [15].

In addition to the rate of recovery from desensitization, the onset of receptor desensitization also influences post-synaptic responses. Blocking AMPA receptor desensitization with cyclothiazide broadens both individual mEPSCs [189] and depolarization-evoked EPSCs [15] in horizontal and OFF bipolar cells. However, cyclothiazide has relatively modest effects

on the kinetics of horizontal cell light responses [182,189]. The main effects of cyclothiazide are to depolarize horizontal cells by enhancing effects of tonic glutamate in the cleft and to increase the depolarizing overshoot at light offset. This suggests that the kinetics of individual mEPSCs have a stronger influence on horizontal cell response kinetics when release is highly synchronized (e.g., at light offset of cones or in response to a depolarizing test pulse applied pre-synaptically) than when vesicular release is less well synchronized.

Although the vesicles of rods and cones appear to contain similar amounts of glutamate, the mean amplitudes of mEPSCs vary among different post-synaptic neurons [15,50]. This may, in part, reflect different types of glutamate receptors on different post-synaptic cells [180, 187,190], but also differences in diffusional distances from the release site. Unlike the relatively simple active zones of conventional central nervous system synapses, the ribbon synapse involves tortuous invaginations with multiple post-synaptic processes [39,54,55,63] possessing clusters of glutamate receptors situated at varying distances from the ribbon [191, 192]. Glutamate released at a synaptic ribbon diffuses rapidly through the limited volume of the synaptic cleft to reach nearby post-synaptic receptors at relatively high concentrations [40,193]. However, glutamate released from the same ribbon also reaches receptors located on relatively distant flat basal contacts, eliciting from them slow broad synaptic currents whose kinetics encompass a relatively long diffusion path from the ribbon [50].

Glutamate Uptake

Because post-synaptic responses result from the presence of glutamate in the synaptic cleft, glutamate removal influences response kinetics. Glutamate is removed from the photoreceptor synapse by diffusion and uptake by glutamate transporters into glial Müller cells and photoreceptors. A light-induced photoreceptor hyperpolarization slows release and lowers intraterminal calcium levels; concomitantly, extracellular glutamate levels in the synapse are lowered. By impeding glutamate removal from the synapse, glutamate transport inhibitors slow the horizontal cell response at light onset [194]. This is not due to changes in the rate of release, as blocking glutamate transport does not significantly alter the kinetics of exocytosis [16]. Müller glial cells possess glutamate transporters [195], and Müller cell processes ensheath the photoreceptor terminals, thereby preventing glutamate released at one synapse from reaching a neighboring photoreceptor synapse [196,197]. Glutamate transporters are also present pre-synaptically on photoreceptor terminals. Noise analysis indicates that each amphibian cone photoreceptor possesses 10,000–20,000 transporter molecules [198]. Studies of the mammalian rod–rod bipolar cell synapse suggest that transporters are clustered at high density (perhaps 10,000/ μm^2) in the rod terminal near the site of release [199].

The principal glutamate transporter in mammalian cones is EAAT2 (GLT1), whereas EAAT5 is the major subtype in rods [200–202]. EAAT2 and EAAT5 also are present in the outer plexiform layer of salamander retina [201]. The glutamate transporter in mammalian Müller cells is EAAT1 (GLAST); amphibian Müller cells possess both EAAT1 and EAAT2 [195, 201]. GLAST knockout mice exhibit reduced ERG b-waves, suggesting a role for Müller cell transporters in regulating cleft glutamate levels [203]. However, the time to peak and decay times of electrically evoked synaptic responses in rod bipolar cells were not altered in GLAST knockout mice [199], suggesting that post-synaptic response kinetics are more directly regulated by pre-synaptic uptake of glutamate into rods than by uptake into Müller cells. Vandenbranden et al. [204] have proposed that Müller cell transporters play a greater role in maintaining steady state glutamate levels in darkness, whereas photoreceptor transporters are more important for the rapid removal of glutamate during light-evoked hyperpolarization of photoreceptors. Uptake into photoreceptors may also be accelerated by hyperpolarization because of the increased driving force for sodium ions which are co-transported with glutamate [194,201,204,205].

Synaptic Depression and Vesicle Replenishment

Photoreceptor synapses are continuously active in the dark and therefore particularly susceptible to the synaptic depression that accompanies maintained or repetitive stimulation at most synapses. Various pre- and post-synaptic mechanisms can produce synaptic depression (reviewed in [206]). Post-synaptic mechanisms include glutamate receptor saturation and desensitization; pre-synaptic mechanisms include use-dependent inhibition of I_{Ca} and depletion of releasable vesicles. Linear correlations between pre- and post-synaptic measures of release suggest that glutamate receptors are not saturated during strong pre-synaptic stimulation [15]. As discussed earlier, slow rates of recovery from glutamate receptor desensitization in subtypes of OFF bipolar cells that possess KA receptors can contribute significantly to post-synaptic depression [180]. In contrast, the glutamate receptors of AMPA receptor-possessing OFF bipolar cells and horizontal cells recover quickly from receptor desensitization [180,207]. Thus, at synapses with AMPA receptors, pre-synaptic factors make a greater contribution to synaptic depression. Comparisons of pre- and post-synaptic measures of release indicate that >80–90% of the synaptic depression at AMPA receptor synapses is pre-synaptic in origin [207].

I_{Ca} in photoreceptors is regulated by a large number of mechanisms. Use-dependent feedback mechanisms include voltage- and calcium-dependent inhibition of I_{Ca} [140–143], inhibition of cone I_{Ca} by the pre-synaptic actions of glutamate on group III mGluRs [208], inhibition of cone I_{Ca} by vesicular protons [208,209], inhibition of I_{Ca} by vesicular zinc [116,210,211], inhibitory effects of adenosine which can be derived from vesicular ATP [212–214], inhibition of rod I_{Ca} due to chloride efflux mediated by pre-synaptic glutamate transporters [215], inhibition of rod I_{Ca} due to chloride efflux through calcium-activated chloride channels [138], and enhancement of rod I_{Ca} due to K^+ efflux through calcium-activated potassium channels [19]. Various neurotransmitters and neuromodulators also regulate rod and cone I_{Ca} , including nitric oxide [216,217], dopamine [132], cannabinoids [218–220], somatostatin [221], insulin [222], retinoids, and polyunsaturated fats [223]. Feedback from horizontal cells onto cones [224] also modulates I_{Ca} [225]. Possible mechanisms for this feedback include modulation of extracellular proton levels [226–228] and ephaptic mechanisms [229] involving hemigap junctions [230,231]. The various mechanisms regulating I_{Ca} in photoreceptors are reviewed in greater detail elsewhere [4,153].

In studies on rods, which lack many of these feedback mechanisms, and in the presence of HEPES buffer, which blocks proton-related mechanisms, I_{Ca} exhibits little inhibition when using sequential test pulses separated by short intervals [160,207]. For example, two 100-ms test pulses separated by an interval of 100 ms depressed I_{Ca} produced by the second pulse by ~10%. By contrast, the same protocol depressed synaptic release by ~50% [207]. Because of a high cooperativity for calcium at the release mechanism, small reductions in I_{Ca} produce large amounts of synaptic depression at the calyx of Held [232]. However, the relationship between I_{Ca} amplitude and release from photoreceptors does not exhibit this marked cooperativity but is instead nearly linear, suggesting that ~80% of the synaptic depression is not due to I_{Ca} inactivation but instead is due to other mechanisms, most likely depletion of the releasable pool of vesicles [207].

The depression of release recovers at a similar rate in rods and cones with a time constant of ~250 ms [207]. This rate of recovery may contribute to the decrease in synaptic output from amphibian photoreceptors at frequencies above 4 Hz [8]. It is similar to the 210–250 ms needed to prime individual vesicles for release at the bipolar cell synapse [28], suggesting that the priming of vesicles for release may be a major factor limiting the rate of recovery from synaptic depression. The fast initial component of the rod-driven EPSC appears to recover more slowly

than later components of the EPSC, suggesting the possibility of multiple vesicle pools with distinct properties in rods [160].

Conclusions and Future Questions

This review describes a large number of mechanisms that collectively regulate the kinetics of synaptic transmission from rod and cone photoreceptors. These include the dynamics of exocytosis, vesicle replenishment, calcium signaling, and glutamate removal. In response to a brief flash of light, the synaptic impulse response is five to ten times faster in cones than rods [9,14]. Which among these mechanisms are principally responsible for rod/cone differences in the kinetics of light-induced synaptic transmission? The main causal factors governing the reduction in synaptic output during light are: (1) the decline in intracellular calcium resulting in diminished release and (2) the removal of glutamate from the synaptic cleft by glutamate transporters. To assess the combined kinetic effects of these two mechanisms at light onset, we examined the post-synaptic currents in horizontal cells evoked when rods and cones were hyperpolarized from -40 to -70 mV, similar to the change in photoreceptor membrane potential that occurs at light onset (Fig. 3; Thoreson and Cadetti, unpublished observations). Depolarization of rod or cones from -70 to -40 mV evoked a transient EPSC in horizontal cells followed by a small sustained synaptic current. When photoreceptor cells were subsequently hyperpolarized back from -40 to -70 mV, this small sustained current decayed back to baseline. Cone-driven EPSCs decayed ~ 1.5 times faster than rod-driven EPSCs (Fig. 3c). This suggests that in response to light-evoked hyperpolarization, the rates at which (a) calcium levels fall in the terminal, (b) glutamate release diminishes, and (c) glutamate is removed from the synapse differ only modestly between rod and cone synapses. Although properties of I_{Ca} , glutamate diffusion, and glutamate receptors also help to shape post-synaptic responses, there are no systematic rod/cone differences in these properties that can account for faster kinetics at cone synapses. Rates of vesicle replenishment are also similar in rods and cones [207]. By contrast, when stimulated with depolarizing test steps from -70 to -30 , similar to the depolarization of photoreceptors at light offset, the initial component of exocytosis from cones was seven times faster than the initial component of exocytosis from rods [16]. Thus, much of the five to tenfold difference in the kinetics of rod and cone synapses appears to be derived from the ability of cones to release vesicles at faster rates.

There are a number of mechanisms that might contribute to rod/cone differences in the kinetics of exocytosis, including the presence of different exocytotic mechanisms or calcium sensors in rods and cones, differences in the diffusional distance from calcium channels to release sites, and differences in intracellular calcium handling mechanisms. With regard to the latter, rod/cone differences in release kinetics are not explained by the contribution of CICR to synaptic release from rods [136]. Akin to the outer segment in which differences in mechanisms of calcium homeostasis contribute to the ability of cones to respond more rapidly than rods to light [11], differences in intraterminal calcium handling and calcium-dependent enzymes also help to shape differences in the kinetics of release by rods and cones.

Many questions concerning photoreceptor ribbon synapses remain unanswered [4,5,56]. For example, does slow synaptic transmission from rods simply permit a better match to the kinetics of the rod light response or have rods sacrificed speed for sensitivity? More specifically, does amplification of release from rods by CICR or other mechanisms enhance sensitivity at rod synapses to small changes in light intensity? Do spatially or physically distinct vesicle pools contribute to sustained and transient components of the EPSC? How are small changes in intensity encoded by changes in release rate that can be reliably detected by post-synaptic cells? What are the functional consequences of the unusually low single channel conductance and open probability of the rod calcium channel, CaV1.4? What are the functional consequences of the unusually high sensitivity to calcium of the release apparatus? Is there one calcium sensor

or two employed at photoreceptor synapses? What is the molecular identity of the sensor(s)? What is the role of the ribbon in release? Photoreceptor synapses possess many of the same synaptic proteins and exhibit many of the same properties as other ribbon and conventional synapses, but the constraints imposed by graded signaling and the need to accurately encode small voltage changes have led to specific adaptations of the synaptic machinery employed at rod and cone synapses.

Acknowledgements

This work was supported by NIH grant EY10542 and Research to Prevent Blindness. I thank Katalin Rabl and Lucia Cadetti for their helpful comments and discussion.

References

1. Arshavsky VY, Lamb TD, Pugh EN Jr. G proteins and phototransduction. *Annu Rev Physiol* 2002;64:153–187. [PubMed: 11826267]
2. Burns ME, Baylor DA. Activation, deactivation, and adaptation in vertebrate photoreceptor cells. *Annu Rev Neurosci* 2001;24:779–805. [PubMed: 11520918]
3. Barnes S. After transduction: response shaping and control of transmission by ion channels of the photoreceptor inner segments. *Neuroscience* 1994;58:447–459. [PubMed: 7513385]
4. Heidelberger R, Thoreson WB, Witkovsky P. Synaptic transmission at retinal ribbon synapses. *Prog Retin Eye Res* 2005;24:682–720. [PubMed: 16027025]
5. Sterling P, Matthews G. Structure and function of ribbon synapses. *Trends Neurosci* 2005;28:20–29. [PubMed: 15626493]
6. tom Dieck S, Brandstätter JH. Ribbon synapses of the retina. *Cell Tissue Res* 2006;326:339–346. [PubMed: 16775698]
7. Baylor DA, Hodgkin AL. Detection and resolution of visual stimuli by turtle photoreceptors. *J Physiol (Lond)* 1973;234:163–198. [PubMed: 4766219]
8. Pasino E, Marchiafava PL. Transfer properties of rod and cone cells in the retina of the tiger salamander. *Vision Res* 1976;16:381–386. [PubMed: 941414]
9. Schnapf JL, Copenhagen DR. Differences in the kinetics of rod and cone synaptic transmission. *Nature* 1982;296:862–864. [PubMed: 6280070]
10. Nowak LM, Green DG. Flicker fusion characteristics of rod photoreceptors in the toad. *Vision Res* 1983;23:845–849. [PubMed: 6415914]
11. Korenbrot JI, Rebrik TI. Tuning outer segment Ca^{2+} homeostasis to phototransduction in rods and cones. *Adv Exp Med Biol* 2002;514:179–203. [PubMed: 12596922]
12. Witkovsky P, Stone S. Rod and cone inputs to bipolar and horizontal cells of the *Xenopus* retina. *Vision Res* 1983;23:1251–1258. [PubMed: 6659374]
13. Baylor DA, Fettiplace R. Transmission from photoreceptors to ganglion cells in turtle retina. *J Physiol (Lond)* 1977;271:391–448. [PubMed: 200736]
14. Copenhagen DR, Ashmore JF, Schnapf JK. Kinetics of synaptic transmission from photoreceptors to horizontal and bipolar cells in turtle retina. *Vision Res* 1983;23:363–369. [PubMed: 6308900]
15. Cadetti L, Tranchina D, Thoreson WB. A comparison of release kinetics and glutamate receptor properties in shaping rod-cone differences in EPSC kinetics in the salamander retina. *J Physiol (Lond)* 2005;569:773–788. [PubMed: 16223761]
16. Rabl K, Cadetti L, Thoreson WB. Kinetics of exocytosis is faster in cones than rods. *J Neurosci* 2005;25:4633–4640. [PubMed: 15872111]
17. Heidelberger R. Electrophysiological approaches to the study of neuronal exocytosis and synaptic vesicle dynamics. *Rev Physiol Biochem Pharmacol* 2001;143:1–80. [PubMed: 11428263]
18. Barnes S, Deschenes MC. Contribution of Ca and Ca-activated Cl channels to regenerative depolarization and membrane bistability of cone photoreceptors. *J Neurophysiol* 1992;68:745–755. [PubMed: 1331354]
19. Xu JW, Slaughter MM. Large-conductance calcium-activated potassium channels facilitate transmitter release in salamander rod synapse. *J Neurosci* 2005;25:7660–7668. [PubMed: 16107652]

20. Barnes S, Hille B. Ionic channels of the inner segment of tiger salamander cone photoreceptors. *J Gen Physiol* 1989;94:719–743. [PubMed: 2482325]
21. Moriondo A, Pelucchi B, Rispoli G. Calcium-activated potassium current clamps the dark potential of vertebrate rods. *Eur J Neurosci* 2001;14:19–26. [PubMed: 11488945]
22. Thoreson WB, Bryson EJ, Rabl K. Reciprocal interactions between calcium and chloride in rod photoreceptors. *J Neurophysiol* 2003;90:1747–1753. [PubMed: 12724369]
23. Thoreson WB, Rabl K, Townes-Anderson E, Heidelberger R. A highly Ca^{2+} -sensitive pool of vesicles contributes to linearity at the rod photoreceptor ribbon synapse. *Neuron* 2004;42:595–605. [PubMed: 15157421]
24. Rieke F, Schwartz EA. Asynchronous transmitter release: control of exocytosis and endocytosis at the salamander rod synapse. *J Physiol (Lond)* 1996;493:1–8. [PubMed: 8735690]
25. von Gersdorff H, Matthews G. Inhibition of endocytosis by elevated internal calcium in a synaptic terminal. *Nature* 1994;370:652–655. [PubMed: 8065451]
26. Thoreson WB, Witkovsky P. Glutamate receptors and circuits in the vertebrate retina. *Prog Retin Eye Res* 1999;18:765–810. [PubMed: 10530751]
27. Rea R, Li J, Dharia A, Levitan ES, Sterling P, Kramer RH. Streamlined synaptic vesicle cycle in cone photoreceptor terminals. *Neuron* 2004;4:755–766. [PubMed: 15003175]
28. Zenisek D, Steyer JA, Almers W. Transport, capture and exocytosis of single synaptic vesicles at active zones. *Nature* 2000;406:849–854. [PubMed: 10972279]
29. Mennerick S, Matthews G. Ultrafast exocytosis elicited by calcium current in synaptic terminals of retinal bipolar neurons. *Neuron* 1996;17:1241–1249. [PubMed: 8982170]
30. Moser T, Beutner D. Kinetics of exocytosis and endocytosis at the cochlear inner hair cell afferent synapse of the mouse. *Proc Natl Acad Sci U S A* 2000;97:883–888. [PubMed: 10639174]
31. Baylor DA, Hodgkin AL, Lamb TD. The electrical response of turtle cones to flashes and steps of light. *J Physiol (Lond)* 1974;242:685–727. [PubMed: 4449052]
32. Burkhardt DA, Fahey PK, Sikora MA. Retinal bipolar cells: contrast encoding for sinusoidal modulation and steps of luminance contrast. *Vis Neurosci* 2004;21:883–893. [PubMed: 15733343]
33. Tranchina D, Gordon J, Shapley R, Toyoda J. Distribution of synaptic markers in the retina: implications for synaptic vesicle traffic in ribbon synapses. *Proc Natl Acad Sci U S A* 1994;78:6540–6542. [PubMed: 6947242]
34. Ashmore JF, Copenhagen DR. An analysis of transmission from cones to hyperpolarizing bipolar cells in the retina of the turtle. *J Physiol (Lond)* 1983;340:569–597. [PubMed: 6310101]
35. Berntson A, Taylor WR. The unitary event amplitude of mouse retinal on-cone bipolar cells. *Vis Neurosci* 2003;20:621–626. [PubMed: 15088715]
36. Choi SY, Borghuis BG, Rea R, Levitan ES, Sterling P, Kramer RH. Encoding light intensity by the cone photoreceptor synapse. *Neuron* 2005;48:555–562. [PubMed: 16301173]
37. Schein S, Ahmad KM. A clockwork hypothesis: synaptic release by rod photoreceptors must be regular. *Biophys J* 2005;89:3931–3949. [PubMed: 16169984]
38. Schein S, Ahmad KM. Efficiency of synaptic transmission of single-photon events from rod photoreceptor to rod bipolar dendrite. *Biophys J* 2006;91:3257–3267. [PubMed: 16920838]
39. Haverkamp S, Grunert U, Wässle H. The cone pedicle, a complex synapse in the retina. *Neuron* 2000;27:85–95. [PubMed: 10939333]
40. Migdale K, Herr S, Klug K, Ahmad K, Linberg K, Sterling P, Schein S. Two ribbon synaptic units in rod photoreceptors of macaque, human, and cat. *J Comp Neurol* 2003;455:100–112. [PubMed: 12454999]
41. Hirasawa H, Shiells R, Yamada M. Analysis of spontaneous EPSCs in retinal horizontal cells of the carp. *Neurosci Res* 2001;40:75–86. [PubMed: 11311408]
42. Attwell D, Borges S, Wu SM, Wilson M. Signal clipping by the rod output synapse. *Nature* 1987;328:522–524. [PubMed: 3039370]
43. Hornstein EP, Verweij J, Li PH, Schnapf JL. Gap-junctional coupling and absolute sensitivity of photoreceptors in macaque retina. *J Neurosci* 2005;25:11201–11209. [PubMed: 16319320]
44. Zhang J, Wu SM. Physiological properties of rod photoreceptor electrical coupling in the tiger salamander retina. *J Physiol (Lond)* 2005;564:849–862. [PubMed: 15746168]

45. Tessier-Lavigne M, Attwell D. The effect of photoreceptor coupling and synapse nonlinearity on signal:noise ratio in early visual processing. *Proc R Soc Lond B Biol Sci* 1988;234:171–197. [PubMed: 2905460]
46. Lebedev DS, Byzov AL, Govardovskii VI. Photoreceptor coupling and boundary detection. *Vision Res* 1998;38:3161–3169. [PubMed: 9893823]
47. DeVries SH, Qi X, Smith R, Makous W, Sterling P. Electrical coupling between mammalian cones. *Curr Biol* 2002;12:1900–1907. [PubMed: 12445382]
48. Armstrong-Gold CE, Rieke F. Bandpass filtering at the rod to second-order cell synapse in salamander (*Ambystoma tigrinum*) retina. *J Neurosci* 2003;23:3796–3806. [PubMed: 12736350]
49. Detwiler PB, Hodgkin AL, McNaughton PA. A surprising property of electrical spread in the network of rods in the turtle's retina. *Nature* 1978;274:562–565. [PubMed: 672987]
50. DeVries SH, Li W, Saszik S. Parallel processing in two transmitter microenvironments at the cone photoreceptor synapse. *Neuron* 2006;50:735–748. [PubMed: 16731512]
51. Krizaj D, Gabriel R, Owen WG, Witkovsky P. Dopamine D2 receptor-mediated modulation of rod-cone coupling in the *Xenopus* retina. *J Comp Neurol* 1998;398:529–538. [PubMed: 9717707]
52. Pyle JL, Kavalali ET, Piedras-Renteria ES, Tsien RW. Rapid reuse of readily releasable pool vesicles at hippocampal synapses. *Neuron* 2000;28:221–231. [PubMed: 11086996]
53. Richards DA, Guatimosim C, Rizzoli SO, Betz WJ. Synaptic vesicle pools at the frog neuromuscular junction. *Neuron* 2003;39:529–541. [PubMed: 12895425]
54. Dowling JE, Werblin FS. Organization of the retina of the mudpuppy, *Necturus maculosus*. I. Synaptic structure. *J Neurophysiol* 1969;32:315–338. [PubMed: 5787842]
55. Lasansky A. Organization of the outer synaptic layer in the retina of the larval tiger salamander. *Phil Trans R Soc B* 1973;265:471–489. [PubMed: 4147132]
56. Prescott ED, Zenisek D. Recent progress towards understanding the synaptic ribbon. *Curr Opin Neurobiol* 2005;15:43143–43146.
57. Saviane C, Silver RA. Fast vesicle reloading and a large pool sustain high bandwidth transmission at a central synapse. *Nature* 2006;439:983–987. [PubMed: 16496000]
58. Pierantoni, RL.; McCann, GD. A quantitative study on synaptic ribbons in the photoreceptors of turtle and frog. In: Borsellino, A.; Cervetto, L., editors. *Photoreceptors*. Plenum; New York: 1981. p. 255–283.
59. Townes-Anderson E, MacLeish PR, Raviola E. Rod cells dissociated from mature salamander retina: ultrastructure and uptake of horseradish peroxidase. *J Cell Biol* 1985;100:175–188. [PubMed: 3965470]
60. Raviola E, Gilula NB. Intramembrane organization of specialized contacts in the outer plexiform layer of the retina. *J Cell Biol* 1975;75:192–222. [PubMed: 1127010]
61. Matsumura M, Okinami S, Ohkuma M. Synaptic vesicle exocytosis in goldfish photoreceptor cells. *Albrecht Von Graefes Arch Klin Exp Ophthalmol* 1981;215:159–170. [PubMed: 6908465]
62. Schaeffer SF, Raviola E, Heuser JE. Membrane specializations in the outer plexiform layer of the turtle retina. *J Comp Neurol* 1982;204:253–267. [PubMed: 6276452]
63. Rao-Mirotnik R, Harkins AB, Buchsbaum G, Sterling P. Mammalian rod terminal: architecture of a binary synapse. *Neuron* 1995;14:561–569. [PubMed: 7695902]
64. Lenzi D, von Gersdorff H. Structure suggests function: the case for synaptic ribbons as exocytotic nanomachines. *BioEssays* 2001;23:831–840. [PubMed: 11536295]
65. Parsons TD, Sterling P. Synaptic ribbon. Conveyor belt or safety belt? *Neuron* 2003;37:379–382. [PubMed: 12575947]
66. Nouvian R, Beutner D, Parsons TD, Moser T. Structure and function of the hair cell ribbon synapse. *J Membr Biol* 2006;209:153–165. [PubMed: 16773499]
67. Moser T, Brandt A, Lysakowski A. Hair cell ribbon synapses. *Cell Tissue Res* 2006;326:347–359. [PubMed: 16944206]
68. Kolb H. Organization of the outer plexiform layer of the primate retina: electron microscopy of Golgi-impregnated cells. *Philos Trans R Soc Lond B* 1970;258:261–283.
69. Lasansky A. Cell junctions at the outer synaptic layer of the retina. *Invest Ophthalmol* 1972;11:265–275. [PubMed: 4112852]

70. Dowling, JE. The retina: an approachable part of the brain. Belknap; Cambridge, MA: 1987.
71. Zenisek D, Davila V, Wan L, Almers W. Imaging calcium entry sites and ribbon structures in two presynaptic cells. *J Neurosci* 2003;23:2538–2548. [PubMed: 12684438]
72. von Gersdorff H. Synaptic ribbons: versatile signal transducers. *Neuron* 2001;29:7–10. [PubMed: 11182076]
73. VonKriegstein K, Schmitz F, Link E, Sudhof TC. Distribution of synaptic vesicle proteins in the mammalian retina identifies obligatory and facultative components of ribbon synapses. *Eur J Neurosci* 1999;11:1335–1348. [PubMed: 10103129]
74. VonKriegstein K, Schmitz F. The expression pattern and assembly profile of synaptic membrane proteins in ribbon synapses of the developing mouse retina. *Cell Tissue Res* 2003;311:159–173. [PubMed: 12596036]
75. Sherry DM, Yang H, Standifer KM. Vesicle-associated membrane protein isoforms in the tiger salamander retina. *J Comp Neurol* 2001;431:424–436. [PubMed: 11223812]
76. Sherry DM, Wang MM, Frishman LJ. Differential distribution of vesicle associated membrane protein isoforms in the mouse retina. *Mol Vis* 2003;9:673–688. [PubMed: 14685145]
77. Morgans CW, Brandstatter JH, Kellerman J, Betz H, Wassle H. A SNARE complex containing syntaxin 3 is present in ribbon synapses of the retina. *J Neurosci* 1996;16:6713–6721. [PubMed: 8824312]
78. Morgans CW. Presynaptic proteins of ribbon synapses in the retina. *Microsc Res Tech* 2000;50:141–150. [PubMed: 10891878]
79. Brandstatter JH, Lohrke S, Morgans CW, Wassle H. Distributions of two homologous synaptic vesicle proteins, synaptoporin and synaptophysin, in the mammalian retina. *J Comp Neurol* 1996;370:1–10. [PubMed: 8797152]
80. Brandstatter JH, Wassle H, Betz H, Morgans CW. The plasma membrane protein SNAP-25, but not syntaxin, is present at photoreceptor and bipolar cell synapses in the rat retina. *Eur J Neurosci* 1996;8:823–828. [PubMed: 9081634]
81. Wang Y, Okamoto M, Schmitz F, Hofmann K, Sudhof TC. Rim is a putative Rab3 effector in regulating synaptic-vesicle fusion. *Nature* 1997;388:593–598. [PubMed: 9252191]
82. Ullrich B, Sudhof TC. Distribution of synaptic markers in the retina: implications for synaptic vesicle traffic in ribbon synapses. *J Physiol (Paris)* 1994;88:249–257. [PubMed: 7874086]
83. Sherry DM, Mitchell R, Standifer KM, du Plessis B. Distribution of plasma membrane-associated syntaxins 1 through 4 indicates distinct trafficking functions in the synaptic layers of the mouse retina. *BMC Neurosci* 2006;7:54. [PubMed: 16839421]
84. Rizo J, Chen X, Arac D. Unraveling the mechanisms of synaptotagmin and SNARE function in neurotransmitter release. *Trends Cell Biol* 2006;16:339–350. [PubMed: 16698267]
85. tom Dieck S, Altmann WD, Kessels MM, Qualmann B, Regus H, Brauner D, Fejtova A, Bracko O, Gundelfinger ED, Brandstatter JH. Molecular dissection of the photoreceptor ribbon synapse: physical interaction of Bassoon and RIBEYE is essential for the assembly of the ribbon complex. *J Cell Biol* 2005;168:825–836. [PubMed: 15728193]
86. Takao-Rikitsu E, Mochida S, Inoue E, Deguchi-Tawarada M, Inoue M, Ohtsuka T, Takai Y. Physical and functional interaction of the active zone proteins, CAST, RIM1, and Bassoon, in neurotransmitter release. *J Cell Biol* 2004;164:301–311. [PubMed: 14734538]
87. Deguchi-Tawarada M, Inoue E, Takao-Rikitsu E, Inoue M, Kitajima I, Ohtsuka T, Takai Y. Active zone protein CAST is a component of conventional and ribbon synapses in mouse retina. *J Comp Neurol* 2006;495:480–496. [PubMed: 16485285]
88. Dick O, Hack I, Altmann WD, Garner CC, Gundelfinger ED, Brandstatter JH. Localization of the presynaptic cytomatrix protein piccolo at ribbon and conventional synapses in the rat retina: comparison with bassoon. *J Comp Neurol* 2001;439:224–234. [PubMed: 11596050]
89. Dick O, tomDieck S, Altmann WD, Ammermuller J, Weiler R, Garner CC, Gundelfinger EK, Brandstatter JH. The presynaptic active zone protein bassoon is essential for photoreceptor ribbon synapse formation in the retina. *Neuron* 2003;37:775–786. [PubMed: 12628168]
90. Mandell JW, Townes-Anderson E, Czernik AJ, Cameron R, Greengard P, DeCamilli P. Synapsins in the vertebrate retina: absence from ribbon synapses and heterogeneous distribution among conventional synapses. *Neuron* 1990;5:19–33. [PubMed: 2114884]

91. Mandell JW, Czernik AJ, de Camilli P, Greengard P, Townes-Anderson E. Differential expression of synapsins I and II among rat retinal synapses. *J Neurosci* 1992;12:1736–1749. [PubMed: 1578266]
92. Greengard P, Benfenati F, Valtorta F. Synapsin I, an actin-binding protein regulating synaptic vesicle traffic in the nerve terminal. *Adv Second Messenger Phosphoprot Res* 1994;29:31–45.
93. Sudhof TC. The synaptic vesicle cycle. *Annu Rev Neurosci* 2004;27:509–547. [PubMed: 15217342]
94. Zenisek D, Horst NK, Merrifield C, Sterling P, Matthews G. Visualizing synaptic ribbons in the living cell. *J Neurosci* 2004;24:9752–9759. [PubMed: 15525760]
95. Schmitz F, Konigstorfer A, Sudhof TC. RIBEYE, a component of synaptic ribbons: a protein's journey through evolution provides insight into synaptic ribbon function. *Neuron* 2000;28:857–872. [PubMed: 11163272]
96. Corda D, Colanzi A, Luini A. The multiple activities of CtBP/BARS proteins: the Golgi view. *Trends Cell Biol* 2006;16:167–173. [PubMed: 16483777]
97. Kondo S, Sato-Yoshitake R, Noda Y, Aizawa H, Nakata T, Matsuura Y, Hirokawa N. KIF3A is a new microtubule-based anterograde motor in the nerve axon. *J Cell Biol* 1994;125:1095–1107. [PubMed: 7515068]
98. Hirokawa N, Takemura R. Kinesin superfamily proteins and their various functions and dynamics. *Exp Cell Res* 2004;301:50–59. [PubMed: 15501445]
99. Muresan V, Lyass A, Schnapp BJ. The kinesin motor KIF3A is a component of the presynaptic ribbon in vertebrate photoreceptors. *J Neurosci* 1999;19:1027–1037. [PubMed: 9920666]
100. Wang MM, Janz R, Belizaire R, Frishman LJ, Sherry DM. Differential distribution and developmental expression of synaptic vesicle protein 2 isoforms in the mouse retina. *J Comp Neurol* 2003;460:106–122. [PubMed: 12687700]
101. Lazzell DR, Belizaire R, Thakur P, Sherry DM, Janz R. SV2B regulates synaptotagmin 1 by direct interaction. *J Biol Chem* 2004;279:52124–52131. [PubMed: 15466855]
102. Schivell AE, Mochida S, Kensel-Hammes P, Custer KL, Bajjalieh SM. SV2A and SV2C contain a unique synaptotagmin-binding site. *Mol Cell Neurosci* 2005;29:56–64. [PubMed: 15866046]
103. Custer KL, Austin NS, Sullivan JM, Bajjalieh SM. Synaptic vesicle protein 2 enhances release probability at quiescent synapses. *J Neurosci* 2006;26:1303–1313. [PubMed: 16436618]
104. Lynch BA, Lambeng N, Nocka K, Kensel-Hammes P, Bajjalieh SM, Matagne A, Fuks B. The synaptic vesicle protein SV2A is the binding site for the antiepileptic drug levetiracetam. *Proc Natl Acad Sci U S A* 2004;101:9861–9866. [PubMed: 15210974]
105. Sherry DM, Heidelberger R. Distribution of proteins associated with synaptic vesicle endocytosis in the mouse and goldfish retina. *J Comp Neurol* 2005;484:440–457. [PubMed: 15770653]
106. Berntson AK, Morgans CW. Distribution of the presynaptic calcium sensors, synaptotagmin I/II and synaptotagmin III, in the goldfish and rodent retinas. *J Vis* 2003;3:274–280. [PubMed: 12803536]
107. Heidelberger R, Wang MM, Sherry DM. Differential distribution of synaptotagmin immunoreactivity among synapses in the goldfish, salamander, and mouse retina. *Vis Neurosci* 2003;20:37–49. [PubMed: 12699082]
108. Roux I, Safieddine S, Nouvian R, Grati M, Simmler MC, Bahloul A, Perfettini I, Le Gall M, Rostaing P, Hamard G, Triller A, Avan P, Moser T, Petit C. Otoferlin, defective in a human deafness form, is essential for exocytosis at the auditory ribbon synapse. *Cell* 2006;127:277–289. [PubMed: 17055430]
109. Heidelberger R, Heinemann C, Neher E, Matthews G. Calcium dependence of the rate of exocytosis in a synaptic terminal. *Nature* 1994;371:513–515. [PubMed: 7935764]
110. Beutner D, Voets T, Neher E, Moser T. Calcium dependence of exocytosis and endocytosis at the cochlear inner hair cell afferent synapse. *Neuron* 2001;29:681–690. [PubMed: 11301027]
111. Rabl K, Thoreson WB. Calcium-dependence of exocytosis in rods and cones. *Soc Neurosci Abstracts* 2005;381:8.
112. Kreft M, Krizaj D, Grilc S, Zorec R. Properties of exocytotic response in vertebrate photoreceptors. *J Neurophysiol* 2003;90:218–225. [PubMed: 12660355]
113. Heidelberger R. Adenosine triphosphate and the late steps in calcium-dependent exocytosis at a ribbon synapse. *J Gen Physiol* 1998;111:225–241. [PubMed: 9450941]

114. Rouze NC, Schwartz EA. Continuous and transient vesicle cycling at a ribbon synapse. *J Neurosci* 1998;18:8614–8624. [PubMed: 9786969]
115. Lou X, Scheuss V, Schneggenburger R. Allosteric modulation of the presynaptic Ca²⁺ sensor for vesicle fusion. *Nature* 2005;435:497–501. [PubMed: 15917809]
116. Cadetti L, Thoreson WB, Piccolino M. Pre- and post-synaptic effects of manipulating surface charge with divalent cations at the photoreceptor synapse. *Neuroscience* 2004;129:791–801. [PubMed: 15541900]
117. Dunlap K, Luebke JI, Turner TJ. Exocytotic Ca²⁺ channels in mammalian central neurons. *Trends Neurosci* 1995;18:89–98. [PubMed: 7537420]
118. Corey DP, Dubinsky JM, Schwartz EA. The calcium current in inner segments of rods from the salamander (*Ambystoma tigrinum*) retina. *J Physiol (Lond)* 1984;354:557–575. [PubMed: 6090654]
119. Wilkinson MF, Barnes S. The dihydropyridine-sensitive calcium channel subtype in cone photoreceptors. *J Gen Physiol* 1996;197:621–630. [PubMed: 8740375]
120. Thoreson WB, Nitzan R, Miller RF. Reducing extracellular Cl⁻ suppresses dihydropyridine-sensitive Ca²⁺ currents and synaptic transmission in amphibian photoreceptors. *J Neurophysiol* 1997;77:2175–2190. [PubMed: 9114264]
121. Schmitz Y, Witkovsky P. Dependence of photoreceptor glutamate release on a dihydropyridine-sensitive calcium channel. *Neuroscience* 1997;78:1209–1216. [PubMed: 9174087]
122. Juusola M, French AS, Uusitalo RO, Weckstrom M. Information processing by graded-potential transmission through tonically active synapses. *Trends Neurosci* 1996;19:292–297. [PubMed: 8799975]
123. Bech-Hansen NT, Naylor MJ, Maybaum TA, Pearce WG, Koop B, Fishman GA, Mets M, Musarella MA, Boycott KM. Loss-of-function mutations in a calcium-channel alpha1-subunit gene in Xp11.23 cause incomplete X-linked congenital stationary night blindness. *Nat Genet* 1998;19:264–267. [PubMed: 9662400]
124. Hoda JC, Zaghetto F, Koschak A, Striessnig J. Congenital stationary night blindness type 2 mutations S229P, G369D, L1068P, and W1440X alter channel gating or functional expression of Ca(v)1.4 L-type Ca²⁺ channels. *J Neurosci* 2005;25:252–259. [PubMed: 15634789]
125. Hoda JC, Zaghetto F, Singh A, Koschak A, Striessnig J. Effects of congenital stationary night blindness type 2 mutations R508Q and L1364H on Cav1.4 L-type Ca²⁺ channel function and expression. *J Neurochem* 2006;96:1648–1658. [PubMed: 16476079]
126. Hemara-Wahanui A, Berjukow S, Hope CI, Dearden PK, Wu SB, Wilson-Wheeler J, Sharp DM, Lundon-Treweek P, Clover GM, Hoda JC, Striessnig J, Marksteiner R, Hering S, Maw MA. A CACNA1F mutation identified in an X-linked retinal disorder shifts the voltage dependence of Cav1.4 channel activation. *Proc Natl Acad Sci U S A* 2005;102:7553–7558. [PubMed: 15897456]
127. Firth SI, Morgan IG, Boelen MK, Morgans CW. Localization of voltage-sensitive L-type calcium channels in the chicken retina. *Clin Exp Ophthalmol* 2001;29:183–187.
128. Morgans CW. Localization of the α 1F calcium channel subunit in the rat retina. *Invest Ophthalmol Vis Sci* 2001;42:2414–2418. [PubMed: 11527958]
129. Morgans CW, Gaughwin P, Maleszka R. Expression of the alpha1F calcium channel subunit by photoreceptors in the rat retina. *Mol Vis* 2001;7:202–209. [PubMed: 11526344]
130. Taylor WR, Morgans C. Localization and properties of voltage-gated calcium channels in cone photoreceptors of *Tupaia belangeri*. *Vis Neurosci* 1998;15:541–552. [PubMed: 9685206]
131. Morgans CW. Calcium channel heterogeneity among cone photoreceptors in the tree shrew retina. *Eur J Neurosci* 1999;11:2989–2993. [PubMed: 10457194]
132. Stella SL Jr, Thoreson WB. Differential modulation of rod and cone calcium currents in tiger salamander retina by D2 dopamine receptors and camp. *Eur J Neurosci* 2000;12:3537–3548. [PubMed: 11029623]
133. Nachman-Clewner M, St Jules R, Townes-Anderson E. L-type calcium channels in the photoreceptor ribbon synapse: localization and role in plasticity. *J Comp Neurol* 1999;415:1–16. [PubMed: 10540354]
134. Steele EC Jr, Chen X, Iuvone PM, MacLeish PR. Imaging of Ca²⁺ dynamics within the presynaptic terminals of salamander rod photoreceptors. *J Neurophysiol* 2005;94:4544–4553. [PubMed: 16107525]

135. Szikra T, Krizaj D. The dynamic range and domain-specific signals of intracellular calcium in photoreceptors. *Neuroscience* 2006;141:143–155. [PubMed: 16682126]
136. Cadetti L, Bryson EJ, Ciccone CA, Rabl K, Thoreson WB. Calcium-induced calcium release in rod photoreceptor terminals boosts synaptic transmission during maintained depolarization. *Eur J Neurosci* 2006;23:2983–2990. [PubMed: 16819987]
137. Nagy AR, Witkovsky P. A freeze-fracture study of synaptogenesis in the distal retina of larval *Xenopus*. *J Neurocytol* 1981;10:897–919. [PubMed: 7310483]
138. Thoreson WB, Nitzan R, Miller RF. Chloride efflux inhibits single calcium channel open probability in vertebrate photoreceptors: chloride imaging and cell-attached patch-clamp recordings. *Vis Neurosci* 2000;17:197–206. [PubMed: 10824674]
139. Doering CJ, Hamid J, Simms B, McRory JE, Zamponi GW. Cav1.4 encodes a calcium channel with low open probability and unitary conductance. *Biophys J* 2005;89:3042–3048. [PubMed: 16085774]
140. Rabl K, Thoreson WB. Calcium-dependent inactivation and depletion of synaptic cleft calcium ions combine to regulate rod calcium currents under physiological conditions. *Eur J Neurosci* 2002;16:2070–2077. [PubMed: 12473074]
141. Baumann L, Gerstner A, Zong X, Biel M, Wahl-Schott C. Functional characterization of the L-type Ca^{2+} channel Cav1.4 α 1 from mouse retina. *Invest Ophthalmol Vis Sci* 2004;45:708–713. [PubMed: 14744918]
142. Koschak A, Reimer D, Walter D, Hoda J-C, Heinzle T, Grabner M, Striessnig J. Cav1.4 α 1 subunits can form slowly inactivating dihydropyridine-sensitive L-type Ca^{2+} channels lacking Ca^{2+} -dependent inactivation. *J Neurosci* 2003;23:6041–6049. [PubMed: 12853422]
143. McRory JE, Hamid J, Doering CJ, Garcia E, Parker R, Hamming K, Chen L, Hildebrand M, Beedle AM, Feldcamp L, Zamponi GW, Snutch TP. The CACNA1F gene encodes an L-type calcium channel with unique biophysical properties and tissue distribution. *J Neurosci* 2004;24:1707–1718. [PubMed: 14973233]
144. Thoreson WB, Tranchina D, Witkovsky P. Kinetics of synaptic transfer from rods and cones to horizontal cells in the salamander retina. *Neuroscience* 2003;122:785–798. [PubMed: 14622921]
145. Ball SL, Powers PA, Shin H-S, Morgans CW, Peachey NS, Gregg RG. Role of the β 2 subunit of voltage-dependent calcium channels in the retinal outer plexiform layer. *Invest Ophthalmol Vis Sci* 2002;43:1595–1603. [PubMed: 11980879]
146. Wycisk KA, Budde B, Feil S, Skosyrski S, Buzzi F, Neidhardt J, Glaus E, Nurnberg P, Ruether K, Berger W. Structural and functional abnormalities of retinal ribbon synapses due to Cacna2d4 mutation. *Invest Ophthalmol Vis Sci* 2006;47:3523–3530. [PubMed: 16877424]
147. Wycisk KA, Zeitz C, Feil S, Wittmer M, Forster U, Neidhardt J, Wissinger B, Zrenner E, Wilke R, Kohl S, Berger W. Mutation in the auxiliary calcium-channel subunit CACNA2D4 causes autosomal recessive cone dystrophy. *Am J Hum Genet* 2006;79:973–977. [PubMed: 17033974]
148. Haeseleer F, Imanishi Y, Maeda T, Possin DE, Maeda A, Lee A, Rieke F, Palczewski K. Essential role of Ca^{2+} -binding protein 4, a Cav1.4 channel regulator, in photoreceptor synaptic function. *Nat Neurosci* 2004;7:1079–1087. [PubMed: 15452577]
149. Maeda T, Lem J, Palczewski K, Haeseleer F. A critical role of CaBP4 in the cone synapse. *Invest Ophthalmol Vis Sci* 2005;46:4320–4327. [PubMed: 16249514]
150. Zeitz C, Kloeckener-Gruissem B, Forster U, Kohl S, Magyar I, Wissinger B, Matyas G, Borruat FX, Schorderet DF, Zrenner E, Munier FL, Berger W. Mutations in CABP4, the gene encoding the Ca^{2+} -binding protein 4, cause autosomal recessive night blindness. *Am J Hum Genet* 2006;79:657–667. [PubMed: 16960802]
151. Singer JH, Diamond JS. Sustained Ca^{2+} entry elicits transient postsynaptic currents at a retinal ribbon synapse. *J Neurosci* 2003;23:10923–10933. [PubMed: 14645488]
152. Klingauf J, Neher E. Modeling buffered Ca^{2+} diffusion near the membrane: implications for secretion in neuroendocrine cells. *Biophys J* 1997;72:674–690. [PubMed: 9017195]
153. Krizaj D, Copenhagen DR. Calcium regulation in photoreceptors. *Front Biosci* 2002;7:2023–2044.
154. Mercurio AM, Holtzman E. Smooth endoplasmic reticulum and other agranular reticulum in frog retinal photoreceptors. *J Neurocytol* 1982;11:263–293. [PubMed: 6978386]

155. Ungar F, Piscopo I, Holtzman E. Calcium accumulation in intracellular compartments of frog retinal rod photoreceptors. *Brain Res* 1981;205:200–206. [PubMed: 6970606]
156. Berridge MJ. The endoplasmic reticulum: a multifunctional signaling organelle. *Cell Calcium* 2002;32:235–249. [PubMed: 12543086]
157. Krizaj D, Lai FA, Copenhagen DR. Ryanodine stores and calcium regulation in the inner segments of salamander rods and cones. *J Physiol (Lond)* 2003;547:761–774. [PubMed: 12562925]
158. Krizaj D, Liu X, Copenhagen DR. Expression of calcium transporters in the retina of the tiger salamander (*Ambystoma tigrinum*). *J Comp Neurol* 2004;475:463–480. [PubMed: 15236230]
159. Krizaj D, Bao JX, Schmitz Y, Witkovsky P, Copenhagen DR. Caffeine-sensitive calcium stores regulate synaptic transmission from retinal rod photoreceptors. *J Neurosci* 1999;19:7249–7261. [PubMed: 10460231]
160. Suryanarayanan A, Slaughter MM. Synaptic transmission mediated by internal calcium stores in rod photoreceptors. *J Neurosci* 2006;26:1759–1766. [PubMed: 16467524]
161. Peng YW, Sharp AH, Snyder SH, Yau KW. Localization of the inositol 1,4,5-trisphosphate receptor in synaptic terminals in the vertebrate retina. *Neuron* 1991;6:525–531. [PubMed: 1849721]
162. Rousseau E, Smith JS, Meissner G. Ryanodine modifies conductance and gating behavior of single Ca^{2+} release channel. *Am J Physiol* 1987;253:C364–C368. [PubMed: 2443015]
163. Pessah IN, Zimanyi I. Characterization of multiple [3H] ryanodine binding sites on the Ca^{2+} release channel of sarcoplasmic reticulum from skeletal and cardiac muscle: evidence for a sequential mechanism in ryanodine action. *Mol Pharmacol* 1991;39:679–689. [PubMed: 1851961]
164. Cadetti L, Bryson EJ, Rabl K, Ciccone C, Thoreson WB. Calcium-induced calcium release (CICR) contributes to glutamate release from rod photoreceptor terminals. *Soc Neurosci Abstract* 2005;45:3.
165. Collin T, Marty A, Llano I. Presynaptic calcium stores and synaptic transmission. *Curr Opin Neurobiol* 2005;15:275–281. [PubMed: 15919193]
166. Lelli A, Perin P, Martini M, Ciubotaru CD, Prigioni I, Valli P, Rossi ML, Mammano F. Presynaptic calcium stores modulate afferent release in vestibular hair cells. *J Neurosci* 2003;23:6894–6903. [PubMed: 12890784]
167. Glowatzki E, Fuchs PA. Transmitter release at the hair cell ribbon synapse. *Nat Neurosci* 2002;5:147–154. [PubMed: 11802170]
168. Singer JH, Lassoova L, Vardi N, Diamond JS. Coordinated multivesicular release at a mammalian ribbon synapse. *Nat Neurosci* 2004;7:826–833. [PubMed: 15235608]
169. Kamishima T, Quayle JM. Ca^{2+} -induced Ca^{2+} release in cardiac and smooth muscle cells. *Biochem Soc Trans* 2003;31:943–946. [PubMed: 14505454]
170. Ramsey IS, Delling M, Clapham DE. An introduction to TRP channels. *Annu Rev Physiol* 2006;68:619–647. [PubMed: 16460286]
171. Krizaj D. Compartmentalization of calcium entry pathways in mouse rods. *Eur J Neurosci* 2005;22:3292–3296. [PubMed: 16367794]
172. Krizaj D, Demarco SJ, Johnson J, Strehler EE, Copenhagen DR. Cell-specific expression of plasma membrane calcium ATPase isoforms in retinal neurons. *J Comp Neurol* 2002;451:1–21. [PubMed: 12209837]
173. Rentería RC, Strehler EE, Copenhagen DR, Krizaj D. Ontogeny of plasma membrane calcium ATPase isoforms in the neural retina of the postnatal rat. *Vis Neurosci* 2005;22:263–274. [PubMed: 16079002]
174. Morgans CW, El Far O, Berntson A, Wassle H, Taylor WR. Calcium extrusion from mammalian photoreceptor terminals. *J Neurosci* 1998;18:2467–2474. [PubMed: 9502807]
175. Hilfiker H, Guerini D, Carafoli E. Cloning and expression of isoform 2 of the human plasma membrane Ca^{2+} ATPase. Functional properties of the enzyme and its splicing products. *J Biol Chem* 1994;269:26178–26183. [PubMed: 7929331]
176. Duncan JL, Yang H, Doan T, Silverstein RS, Murphy GJ, Nune G, Liu X, Copenhagen D, Tempel BL, Rieke F, Krizaj D. Scotopic visual signaling in the mouse retina is modulated by high-affinity plasma membrane calcium extrusion. *J Neurosci* 2006;26:7201–7211. [PubMed: 16822977]

177. Rusakov DA. Ca^{2+} -dependent mechanisms of presynaptic control at central synapses. *Neuroscientist* 2006;12:317–326. [PubMed: 16840708]
178. Kits KS, Mansvelder HD. Regulation of exocytosis in neuroendocrine cells: spatial organization of channels and vesicles, stimulus-secretion coupling, calcium buffers and modulation. *Brain Res Brain Res Rev* 2000;33:78–94. [PubMed: 10967354]
179. Miller RJ. The control of neuronal Ca^{2+} homeostasis. *Prog Neurobiol* 1991;37:255–285. [PubMed: 1947178]
180. DeVries SH. Bipolar cells use kainate and AMPA receptors to filter visual information into separate channels. *Neuron* 2000;28:847–856. [PubMed: 11163271]
181. Dingledine R, Borges K, Bowie D, Traynelis SF. The glutamate receptor ion channels. *Pharmacol Rev* 1999;51:7–61. [PubMed: 10049997]
182. Yang JH, Maple B, Gao F, Maguire G, Wu SM. Postsynaptic responses of horizontal cells in the tiger salamander retina are mediated by AMPA-preferring receptors. *Brain Res* 1998;797:125–134. [PubMed: 9630565]
183. Maple BR, Gao F, Wu SM. Glutamate receptors differ in rod- and cone-dominated off-center bipolar cells. *Neuroreport* 1999;10:3605–3610. [PubMed: 10619652]
184. Kim HG, Miller RF. Rods and cones activate different excitatory amino acid receptors on the mudpuppy retinal horizontal cell. *Brain Res* 1991;538:141–146. [PubMed: 1673359]
185. Kim HG, Miller RF. Properties of synaptic transmission from photoreceptors to bipolar cells in the mudpuppy retina. *J Neurophysiol* 1993;69:352–360. [PubMed: 8384660]
186. Kawai F. Characterization of spontaneous excitatory synaptic currents in newt retinal bipolar cells. *Neurosci Lett* 1999;271:49–52. [PubMed: 10471211]
187. Maple BR, Werblin FS, Wu SM. Miniature excitatory postsynaptic currents in bipolar cells of the tiger salamander retina. *Vision Res* 1994;34:2357–2362. [PubMed: 7975276]
188. Evans EM. On the ultrastructure of the synaptic region of visual receptors in certain vertebrates. *Z Zellforsch* 1966;71:499–516. [PubMed: 5983225]
189. Hirasawa H, Shiells R, Yamada M. Blocking AMPA receptor desensitization prolongs spontaneous EPSC decay times and depolarizes H1 horizontal cells in carp retinal slices. *Neurosci Res* 2001;40:217–225. [PubMed: 11448513]
190. Wu SM, Gao F, Maple BR. Functional architecture of synapses in the inner retina: segregation of visual signals by stratification of bipolar cell axon terminals. *J Neurosci* 2000;20:4462–4470. [PubMed: 10844015]
191. Haverkamp S, Grunert U, Wassle H. Localization of kainate receptors at the cone pedicles of the primate retina. *J Comp Neurol* 2001;436:471–486. [PubMed: 11447590]
192. Haverkamp S, Grunert U, Wassle H. The synaptic architecture of AMPA receptors at the cone pedicle of the primate retina. *J Neurosci* 2001;21:2488–2500. [PubMed: 11264323]
193. Rao-Mirotnik R, Buchsbaum G, Sterling P. Transmitter concentration at a three-dimensional synapse. *J Neurophysiol* 1998;80:3163–3172. [PubMed: 9862914]
194. Gaal L, Roska B, Picaud SA, Wu SM, Marc R, Werblin F. Postsynaptic response kinetics are controlled by a glutamate transporter at cone photoreceptors. *J Neurophysiol* 1998;79:190–196. [PubMed: 9425190]
195. Rauen T, Taylor WR, Kuhlbrodt K, Wiessner M. High-affinity glutamate transporters in the rat retina: a major role of the glial glutamate transporter GLAST-1 in transmitter clearance. *Cell Tissue Res* 1998;291:19–31. [PubMed: 9394040]
196. Sarantis M, Mobbs P. The spatial relationship between Müller cell processes and the photoreceptor output synapse. *Brain Res* 1992;584:299–304. [PubMed: 1325248]
197. Burris C, Klug K, Ngo IT, Sterling P, Schein S. How Müller glial cells in macaque fovea coat and isolate the synaptic terminals of cone photoreceptors. *J Comp Neurol* 2002;453:100–111. [PubMed: 12357435]
198. Larsson HP, Picaud SA, Werblin FS, Lecar H. Noise analysis of the glutamate-activated current in photoreceptors. *Biophys J* 1996;70:733–742. [PubMed: 8789090]
199. Hasegawa J, Obara T, Tanaka K, Tachibana M. High-density presynaptic transporters are required for glutamate removal from the first visual synapse. *Neuron* 2006;50:63–74. [PubMed: 16600856]

200. Rauen T, Kanner BI. Localization of the glutamate transporter GLT-1 in rat and macaque monkey retinae. *Neurosci Lett* 1994;169:137–140. [PubMed: 8047270]
201. Eliasof S, Arriza JL, Leighton BH, Kavanaugh MP, Amara SG. Excitatory amino acid transporters of the salamander retina: identification, localization, and function. *J Neurosci* 1998;18:698–712. [PubMed: 9425012]
202. Pow DV, Barnett NL. Developmental expression of excitatory amino acid transporter 5: a photoreceptor and bipolar cell glutamate transporter in rat retina. *Neurosci Lett* 2000;280:21–24. [PubMed: 10696802]
203. Harada T, Harada C, Watanabe M, Inoue Y, Sakagawa T, Nakayama N, Sasaki S, Okuyama S, Watase K, Wada K, Tanaka K. Functions of the two glutamate transporters GLAST and GLT-1 in the retina. *Proc Natl Acad Sci U S A* 1998;95:4663–4666. [PubMed: 9539795]
204. Vandenbranden CA, Verweij J, Kamerlans M, Muller LJ, Ruijter JM, Vrensen GF, Spekrijse H. Clearance of neurotransmitter from the cone synaptic cleft in goldfish retina. *Vision Res* 1996;36:3859–3874. [PubMed: 9068839]
205. Roska B, Gaal L, Werblin FS. Voltage-dependent uptake is a major determinant of glutamate concentration at the cone synapse: an analytical study. *J Neurophysiol* 1998;80:1951–1960. [PubMed: 9772252]
206. Zucker RS, Regehr WG. Short-term synaptic plasticity. *Annu Rev Physiol* 2002;64:355–405. [PubMed: 11826273]
207. Rabl K, Cadetti L, Thoreson WB. Paired-pulse depression at photoreceptor synapses. *J Neurosci* 2006;26:2555–2563. [PubMed: 16510733]
208. Hosoi N, Arai I, Tachibana M. Group III metabotropic glutamate receptors and exocytosed protons inhibit L-type calcium currents in cones but not in rods. *J Neurosci* 2005;25:4062–4072. [PubMed: 15843608]
209. DeVries SH. Exocytosed protons feedback to suppress the Ca^{2+} current in mammalian cone photoreceptors. *Neuron* 2001;32:1107–1117. [PubMed: 11754841]
210. Akagi T, Kaneda M, Ishii K, Hashikawa T. Differential subcellular localization of zinc in the rat retina. *J Histochem Cytochem* 2001;49:87–96. [PubMed: 11118481]
211. Wu SM, Qiao X, Noebels JL, Yang XL. Localization and modulatory actions of zinc in vertebrate retina. *Vision Res* 1993;33:2611–2626. [PubMed: 8296456]
212. Stella SL Jr, Bryson EJ, Thoreson WB. A_2 adenosine receptors inhibit calcium influx through L-type calcium channels in rod photoreceptors of the tiger salamander retina. *J Neurophysiol* 2002;87:333–350. [PubMed: 11784754]
213. Stella SL Jr, Bryson EJ, Cadetti L, Thoreson WB. Endogenous adenosine reduces glutamatergic output from rods through activation of A_2 -like adenosine receptors. *J Neurophysiol* 2003;90:165–174. [PubMed: 12843308]
214. Stella SL Jr, Hu W, Vila A, Brecha N. Adenosine inhibits voltage-dependent Ca^{2+} influx in cone photoreceptor terminals of the tiger salamander retina. *J Neurosci Res* 2007;85:1126–1137. [PubMed: 17304584]
215. Rabl K, Bryson EJ, Thoreson WB. Activation of glutamate transporters in rods inhibits presynaptic calcium currents. *Vis Neurosci* 2003;20:557–566. [PubMed: 14977334]
216. Kourennyi DE, Liu X, Hart J, Mahmud F, Baldrige WH, Barnes S. Reciprocal modulation of calcium dynamics at rod and cone photoreceptor synapses by nitric oxide. *J Neurophysiol* 2004;92:477–483. [PubMed: 14985410]
217. Kourennyi DE, Moroz LL, Turner RW, Sharkey KA, Barnes S. Modulation of ion channels in rod photoreceptors by nitric oxide. *Neuron* 1994;13:315–324. [PubMed: 7520253]
218. Straiker A, Sullivan JM. Cannabinoid receptor activation differentially modulates ion channels in photoreceptors of the tiger salamander. *J Neurophysiol* 2003;89:2647–2654. [PubMed: 12740409]
219. Fan S-F, Yazulla S. Biphasic modulation of voltage-dependent currents of retinal cones by cannabinoid CB1 receptor agonist WIN 55212-2. *Vis Neurosci* 2003;20:177–188. [PubMed: 12916739]
220. Fan S-F, Yazulla S. Inhibitory interaction of cannabinoid CB1 receptor and dopamine D2 receptor agonists on voltage-gated currents of goldfish cones. *Vis Neurosci* 2004;21:69–77. [PubMed: 15137583]

221. Akopian A, Johnson J, Gabriel R, Brecha N, Witkovsky P. Somatostatin modulates voltage-gated K^+ and Ca^{2+} currents in rod and cone photoreceptors of the salamander retina. *J Neurosci* 2000;20:929–936. [PubMed: 10648697]
222. Stella SL Jr, Bryson EJ, Thoreson WB. Insulin inhibits voltage-dependent calcium influx into rod photoreceptors. *Neuroreport* 2001;12:947–951. [PubMed: 11303766]
223. Vellani V, Reynolds AM, McNaughton PA. Modulation of the synaptic Ca^{2+} current in salamander photoreceptors by polyunsaturated fatty acids and retinoids. *J Physiol (Lond)* 2000;529:333–344. [PubMed: 11101644]
224. Baylor DA, Fuortes MG, O'Bryan PM. Receptive fields of cones in the retina of the turtle. *J Physiol (Lond)* 1971;214:265–294. [PubMed: 5579638]
225. Verweij J, Kamermans M, Spekreijse H. Horizontal cells feed back to cones by shifting the cone calcium-current activation range. *Vision Res* 1996;36:3943–3953. [PubMed: 9068848]
226. Hirasawa H, Kaneko A. pH changes in the invaginating synaptic cleft mediate feedback from horizontal cells to cone photoreceptors by modulating Ca^{2+} channels. *J Gen Physiol* 2003;122:657–671. [PubMed: 14610018]
227. Vessey JP, Stratis AK, Daniels BA, Da Silva N, Jonz MG, Lalonde MR, Baldrige WH, Barnes S. Proton-mediated feedback inhibition of presynaptic calcium channels at the cone photoreceptor synapse. *J Neurosci* 2003;25:4108–4117. [PubMed: 15843613]
228. Cadetti L, Thoreson WB. Feedback effects of horizontal cell membrane potential on cone calcium currents studied with simultaneous recordings. *J Neurophysiol* 2006;95:1992–1995. [PubMed: 16371457]
229. Byzov AL, Shura-Bura TM. Electrical feedback mechanism in the processing of signals in the outer plexiform layer of the retina. *Vision Res* 1986;26:33–44. [PubMed: 3012877]
230. Kamermans M, Fahrenfort I, Schultz K, Janssen-Bienhold U, Sjoerdsma T, Weiler R. Hemichannel-mediated inhibition in the outer retina. *Science* 2001;292:1178–1180. [PubMed: 11349152]
231. Fahrenfort I, Klooster J, Sjoerdsma T, Kamermans M. The involvement of glutamate-gated channels in negative feedback from horizontal cells to cones. *Prog Brain Res* 2005;147:219–229. [PubMed: 15581709]
232. Xu J, Wu LG. The decrease in the presynaptic calcium current is a major cause of short-term depression at a calyx-type synapse. *Neuron* 2005;46:633–645. [PubMed: 15944131]

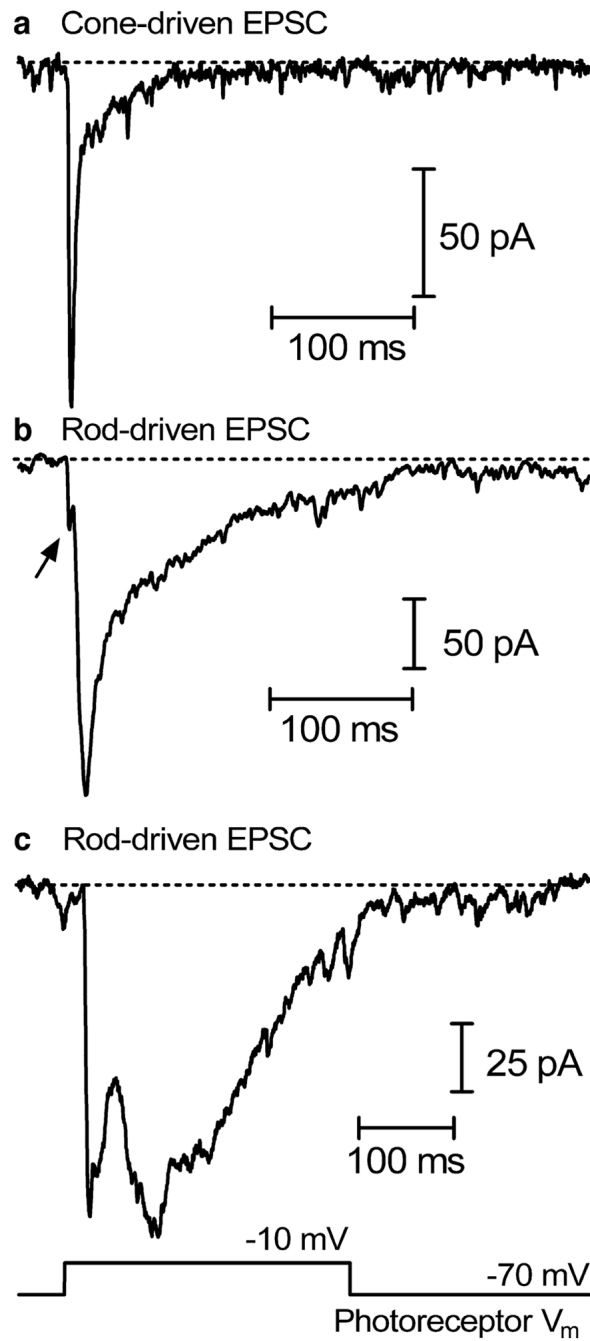


Fig. 1. Examples of EPSCs evoked in horizontal cells by presynaptic stimulation of cones (**a**) and rods (**b**, **c**). The cone-driven EPSC is faster and more transient than the rod-driven EPSCs, but there is also a fast cone-like initial component evident in the rod-driven response shown in **b** (*arrow*). Salamander photoreceptors were stimulated by depolarizing voltage steps from -70 to -10 mV, and horizontal cells were voltage-clamped at -50 mV

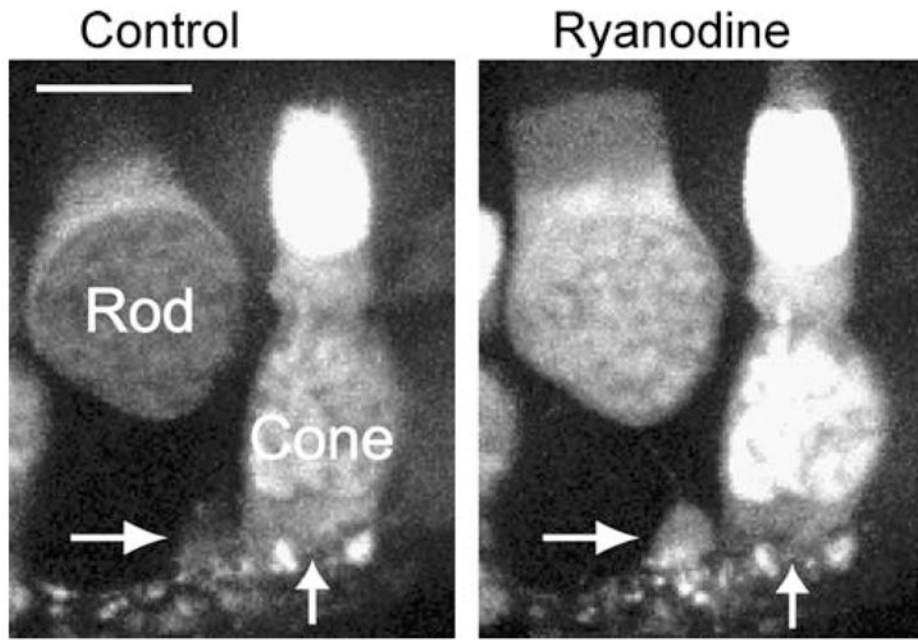
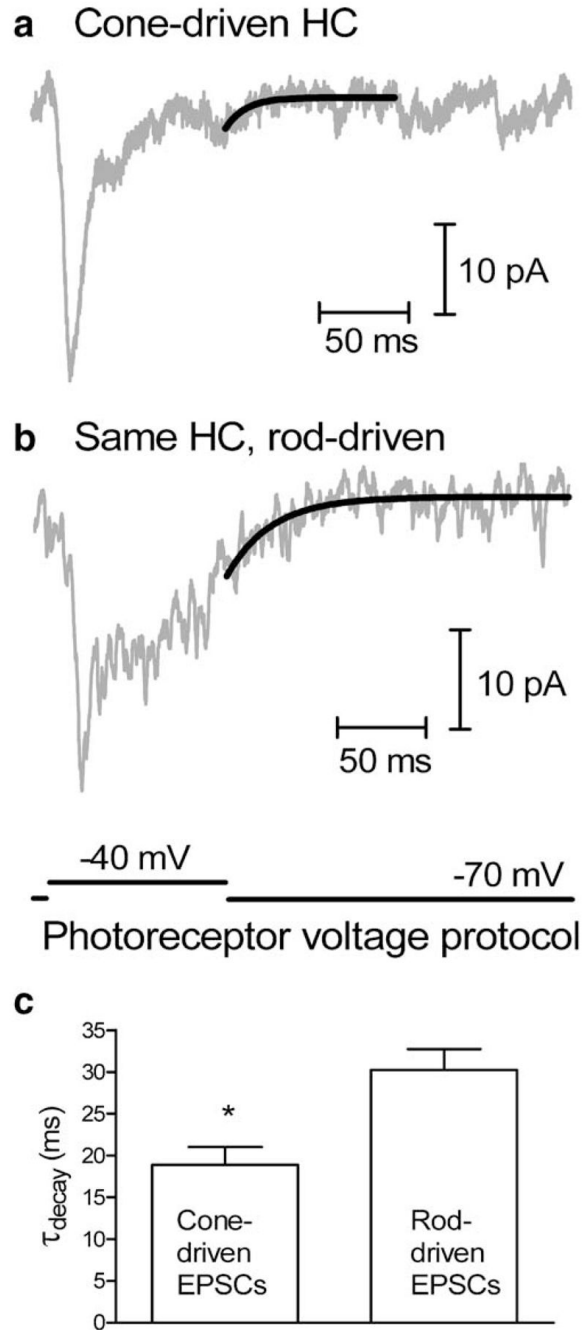


Fig. 2. Ryanodine (1 μM) stimulates Ca^{2+} increases in rods and cones from a salamander retinal slice loaded with the calcium-sensitive dye, fluo-4. Images are stacks of five confocal sections taken at 1- μm intervals. Image acquisition time was 125 ms/confocal slice. The somas of a rod and cone are labeled in the figure. Bath application of ryanodine for 3 min stimulated a Ca^{2+} increase in both the soma and synaptic terminal (*horizontal arrow*) of the rod. Ryanodine also caused a Ca^{2+} increase in the soma of the cone, but not the synaptic region at the base of soma (*vertical arrow*) showed little change. Scale bar=10 μm

**Fig. 3.**

Upon returning to a holding potential of -70 mV after a step to -40 mV, the EPSC evoked in a salamander horizontal cell by presynaptic stimulation of a cone (**a**) decayed more rapidly than the EPSC evoked in the same horizontal cell (HC) by rod stimulation (**b**). **c** Average data from five horizontal cells in which presynaptic test pulses were applied to both a rod and a cone. The EPSCs evoked by cone stimulation ($\tau=18.9$ ms) decayed at a significantly ($P=0.01$) more rapid rate than those evoked in the same horizontal cells by stimulation of rods ($\tau=30.2$ ms). Horizontal cells were voltage-clamped at -50 mV